GJR Publication
OPEN ACCESS

Global Journal of Research in Engineering & Computer Sciences
ISSN: 2583-2727 (Online)
Volume 06 | Issue 02 | March-April | 2026
Journal homepage: https://gjrpublication.com/gjrecs/

Original Research Article

Mathematical-Computational Optimization of UHMWPE Knee Arthroplasty Linear Wear Comparative-Predictions for Archard and Cross-Shear Models

*Francisco Casesnoves

PhD Engineering, MSc Physics-Mathematics, Medical Doctor, Physician. Independent Bioengineering Laboratory, Tallinn, Harjumaa, Baltic States. IAAM member, International Association of Advances Materials, Sweden. Uniscience Global Scientific member, Wyoming, USA.

DOI: 10.5281/zenodo.18919268 **Submission Date: 20 Oct. 2025 | Published Date: 09 March 2026**

Abstract

In previous-recent articles series, linear wear predictions for metal-UHMWPE total knee arthroplasty (TKA) was simulated-optimized for classical Archard's model, with new-updated algorithms. This research improves that publication with the computational intelligence comparative simulation-optimization for Cross-shear model and Archard's one— namely, linear wear. The algorithms for Integer and Integral Formulation are explained. To carry out simulations software, selected literature experimental data, both in vitro and in vivo, is set within programming patterns. 3D Imaging-processing computational simulations software in 3D are designed with Graphical Optimization and Interior Optimization techniques. For [1-5] Million Cycles (Mc) results in Linear Wear, the numerical dataset and 3D simulations image-processing graphs are demonstrated. Then, are compared/discussed for these two models and also to literature database. Useful Biotribology/Biomaterials and Biomedical TKA clinical/manufacturing applications are briefed.

Keywords: *Total knee arthroplasty (TKA), 3D Simulations, Optimization, Linear Wear, Mathematical Model, Load, Sliding Distance, PE (Polyethylene).*

Abbreviations: CSE: Cross-Shear Model, Archard's Model: AM**,** FE: Finite Elements method, K_{wear}: Linear and Volume wear constant, L_{wear}: Linear abrasive wear, Mc: Million cycles, PE: Polyethylene, TKA: Total knee arthroplasty, UHMWPE: Ultra high molecular weight polyethylene.

1.INTRODUCTION AND OBJECTIVES

TKA models are very specific as functions of, among others, anatomical, biomechanical, biodynamics, biotribological and bioenergy proper knee characteristics. For UHMWPE prostheses, the classical Archard's model applied for TKA wear is based on a linear sliding magnitude of the femur TKA-metal condyle along the UHMWPE tibial-part of the prosthesis. In recent years, a cross-shear model was developed taking into account the nonlinear displacement sliding distance of the UHMWPE tibial-part of the prosthesis. That physical phenomenon can cause a cross-shear over the UHMWPE tibial-part of the prosthesis. The most important differences between the classical Archard' s model and the Cross-shear one, [7.0] are given by these characteristics.

1. For Archard's model, sliding distance is a linear magnitude. While for cross-shear model, it is a nonlinear curved displacement, [7.1-7.5].
2. Archard's model do not consider initially the shear phenomenon, while cross-shear one does so.
3. The mathematical equations and algorithmic differences, therefore, between both models are substantially different.
4. The linear wear prediction results, in consequence, different for each model.
5. The cross-shear model usually sets an adimensional wear coefficient, while in AM is implemented a wear factor with proper dimensions, (mm^3 / N mm). However, magnitudes or both are similar, about 10exp (-8, or -9) magnitude order, [7.1,7.2,7.3]. That is, differ in one magnitude order.
6. Fixed-bearing TKA and Rotating-bearing TKA show differences related to contact area [7.1,7.2,7.3,7.7]. This is an important difference between two types of TKA-tibial-plateau component. Contact areas are different, but numerical linear wear predictions with cross-shear models do not differ significantly.

1.1 DIFFICULTIES FOR GETTING STANDARD RESULTS IN TKA WEAR

One important characteristic of TKA along the extensive literature is the large variety of methods, biotribology laboratory apparatus, algorithms, units to present results, and ISO standards [7.6]. Here it is set the most important hurdles to understand and compare the amount techniques and results.

1. **Units:** The most frequently units to present results are mm/Mc for linear wear, and mm3/Mc for volumetric one. The wear magnitudes and rates differ in literature and laboratories for two main reasons: (1) the large variety of testing apparatus and methods, (2) the large variety to communicate/measure results. namely, wear per Mc (mm), wear per year (mm), wear per Mc (mg), wear per year (mg), and others. When the study is in vivo, wear is usually expressed in mm/year. What is common is the polyethylene density approximately equal to water, about 0.96 mg/mm3. Additional complementary dataset and further reading can be found at [7.1-7.7].
2. **Conversion of units:** Although it seems complicated, some techniques can be used to convert undesirable units in any publication results into other ones more convenient if it is the case. When linear/volumetric results are shown in erosion/year, (it could be mm, mm3, or mg), there are references to calculate approximately the number of million cycles (Mc) per year [7.5]. In doing so, an approximation is got to convert mm/year into mm/Mc through statistics of average number of Mc per year [7.5]. For instance, if the results are shown in mg, it is easy to convert taking into account that UHMWPE density is approximately the water one, about 0.96 mg/mm3.
3. **ISO norms variety:** ISO norms are regulated but show many varieties. When comparing experimental and simulation results/datasets it is rather difficult, even if the studies have set the same ISO norms, [7.6].
4. **Different apparatus:** TKA biotribology laboratories use a large amount of different manufactured machines to get trustworthy results [7.5,7.6]. The apparatus differs in output units, design, or mechanical methods to measure erosion. As a result, it is a must to study all those before interpret linear or volumetric TKA erosion dataset.
5. **Different computational methods and models:** The standard method for TKA erosion research is FE. However, the FE variety methods is large. The computational systems are varied, for example, Abaqus or Matlab, [7.1-7.7].

1.2 BIOMECHANICAL RATIONAL-BASE OF CROSS-SHEAR MODEL

At Figures 1,1.1 [7.0], it is shown the biomechanical demonstration of the existence of a shear-force both in natural tibia plateau and the prosthesis one. The forces decomposition and biokinematics/biomechanics are detailed. The shear abrasion increases the total wear magnitude of the TKA prostheses.

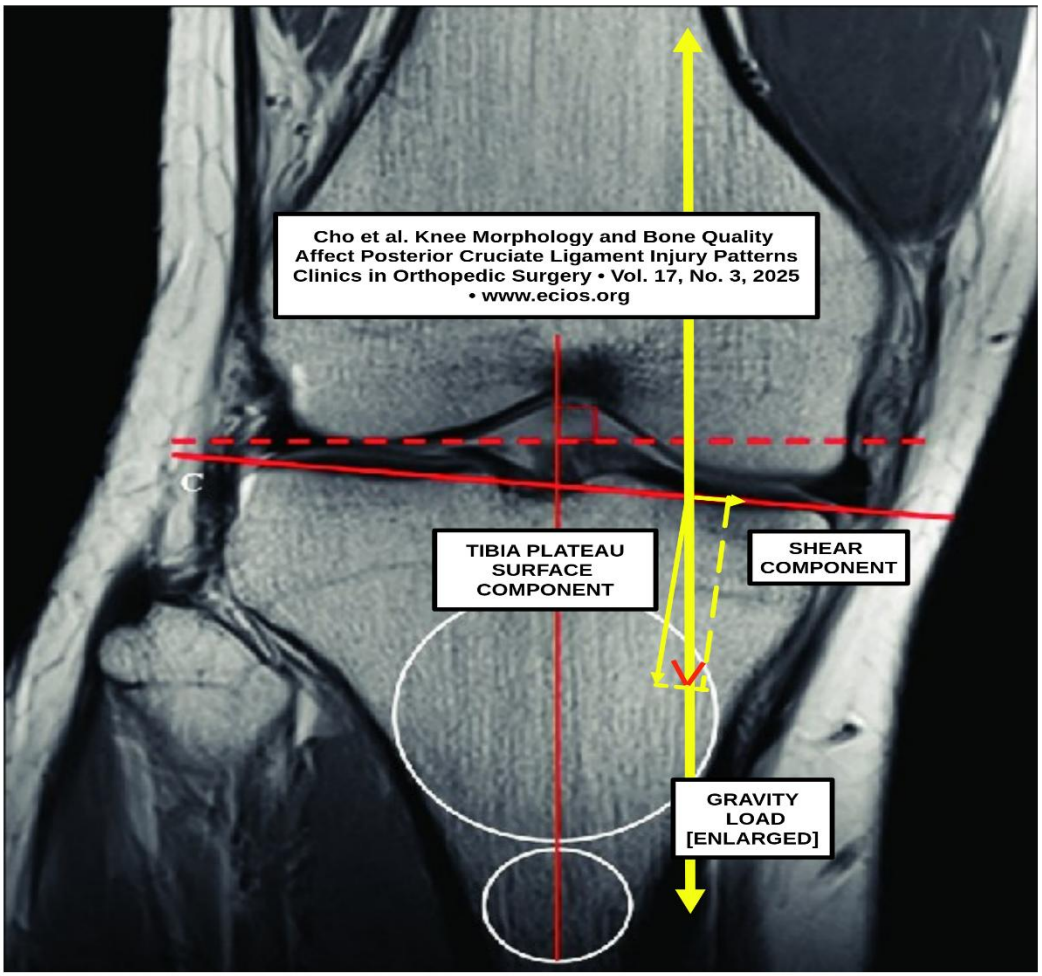

Figure 1: Biomechanical analysis, (coronal (side-to-side) plane), to demonstrate the basis of the cross-shear models. This sketch is modified from a Figure in Google Free images from [Cho et al. Knee Morphology and Bone Quality Affect Posterior Cruciate Ligament Injury Patterns. Clinics in Orthopedic Surgery. Vol. 17, No. 3, 2025. www.ecios.org], in [7.0]. The curvature of the tibial plateau—the upper surface of the shinbone—is asymmetrical, with distinct shapes for the medial (inner) and lateral (outer) sides. These differences are critical for knee stability, biodynamics and biomechanics. Anatomy of curvature: the tibial plateau is divided into two articular surfaces with opposing geometries: medial tibial plateau: It is concave in both the sagittal (front-to-back) and coronal (side-to-side) planes. This "bowl" shape provides a stable seat for the larger medial femoral condyle. Lateral tibial plateau: It is generally convex in the sagittal plane and flat to slightly convex in the coronal plane. This "dome" shape, situated slightly higher (more proximal) than the medial side, allows for the complex rolling and gliding motions of the knee. At sketch, it is shown forces decomposition. Namely, the vertical load, over the bent tibial plateau surface, decomposes into two forces. One lateral, that causes shear in the prosthesis, and a second perpendicular to the plateau surface. Therefore, it is clear that mechanical shear occurs during movement. Archard's classical model considers a sliding path exclusively along the AP or PA directions, omitting the lateral-shear forces/displacements.

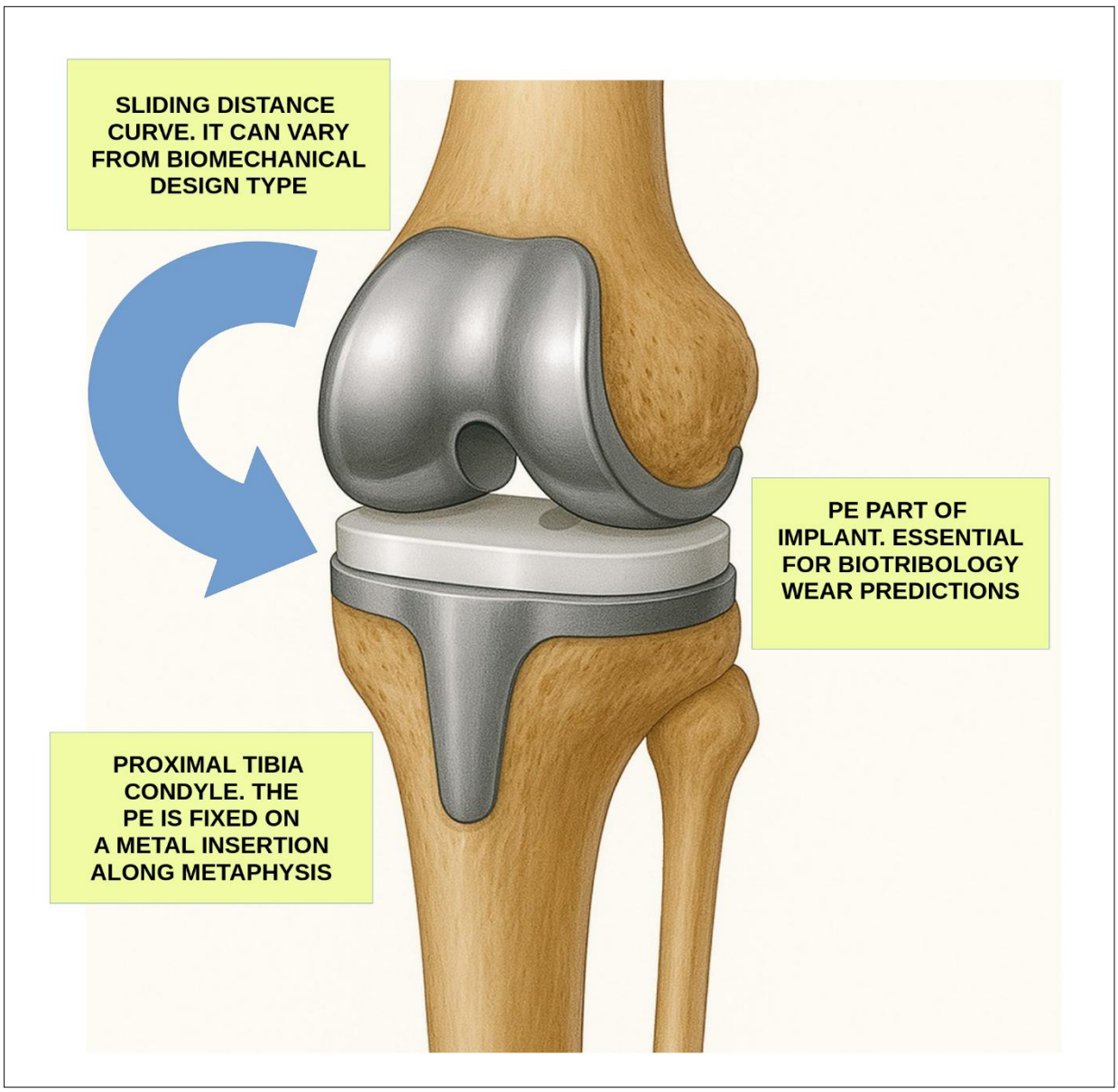

Figure 1.1: [Google free images], modified and drawn by Francisco Casesnoves. The sketch is completed with main parts of TKA. Inset, the most important anatomical parts are marked. Note that the femur condyles are made in steel, and the tibial plateau is polyethylene. More sketchs that illustrate the TKA biomechanics can be found at [7.5].

Therefore, the rationale of this study is to get a precise comparison between these two models. Archard's is classical, but still used, and Cross-Shear is more recent and in general gives higher erosion magnitude orders. It is not an objective of the research to assert any arguments to consider totally superior/inferior any of these models. Instead, the aim is explain and demonstrate sharp differences in algorithms, precision, predictions, and research options when using any of these models. What is biomechanically clear, Figure 1, is that the sliding of the TKA is not a straight line-curve. The method used is Graphical and Interior Optimization software, with specific algorithms. The designed programming is precise and the graphs are intended be sharp and illustrative.

1.3 STUDY OBJECTIVES

Therefore, objectives are mainly two. First and foremost, to design software engineering for computational-simulations and optimization of these two models. Secondly, to evaluate with objective criteria the results differences between the models for linear wear. Complementary biomechanical and biodynamics applications are explained.

In summary, comparative linear wear simulation-optimization research was done with the classical Archard's model and the more recent Cross-shear one. Computational intelligence software was designed for both model algorithms. 2D-3D imaging-processing graphical and interior optimization results agree the most literature results for these models in linear wear. TKA applications are briefed.

2. CROSS-SHEAR AND ARCHARD MODELS FORMULATION

The cross-shear model and its variants can be simulated-optimized with a number of formulas. In general, it is a simpler equation with the exception of the wear coefficient calculation. At Equation (1) is shown the most simple. It is sharply explained the differences between Archard's and Cross-Shear modeling. In general, the cross-shear model is conceived for volumetric wear, although in this study it is optimized for linear wear. Note the difference between the wear factor, and the wear coefficient in Equation (1). The Equations (1,2) and their algorithms have been developed in physics-biomechanics by the Author from literature sources, [7.1,7.5].

$$
\begin{aligned}
&The\ Archard's\ Model\ applied\ on\ TKA,\\
&L_{wear-Archard-Model} \;=\; [\, K_{wear-factor} \,] \sum_{j=1}^{N} \left[\sum_{i=1}^{n} p_i \, |\overrightarrow{v_i}| \, \triangle t_i \right]_j ;\\
&where\ \ K_{wear}\ is\ a\ dimensional\ WEAR\ FACTOR\,;\ N\ is\ cycle\ number\,;\\
&The\ Cross-Shear\ Model\ applied\ on\ TKA,\\
&L_{wear-Cross-Shear-Model} \;=\; [\, K_{wear-coefficient} \,] \sum_{j=1}^{N} \left[\sum_{i=1}^{n} |\overrightarrow{v_i}| \, \triangle t_i \right]_j ;\\
&where\ K_{wear-coefficient}\ is\ an\ adimensional\ and\ K,\\
&is\ WEAR\ COEFFICIENT\,;\ N\ is\ cycle\ number\,;
\end{aligned}
\tag{1}
$$

[Casesnoves Bioengineering Laboratory. Algorithm-development-311]

Where,

Lwear : Linear abrasive wear (mm). It is set for both models in mm.

Kwear-Archard-Model: Wear Factor, standard (mm^3 / N mm). Note: at figures values range of K_w are usually multiplied by 10^{-3}.

Kwear-Cross-Shear-Model: Wear Coefficient, standard (adimensional).

p_i : Pressure (N / mm^2) .

v_i : Sliding discrete Velocity for discrete time increment (mm / s).

Δt_i : Discrete time interval (s).

i, j : Summatory indexes. The [**i**] is for velocity variation within a cycle (n). The [**j**] is for cycles number (N).

3. CROSS-SHEAR MODEL COMPUTATIONAL METHOD

The simplest cross-shear linear wear model is shown in Equation 2. Creep is not implemented for these computational simulation-optimizations. Cross-shear ratio is used to determine the wear coefficient. For linear wear, the use of wear coefficient instead the wear factor simplifies the calculations, [7.1].

$$
\begin{aligned}
&The\ Cross-Shear\ Model\ applied\ on\ TKA,\\
&L_{wear-Cross-Shear-Model} = [\,K_{wear-coefficient}\,] \sum_{j=1}^{N}\left[\sum_{i=1}^{n} |\overrightarrow{v_i}|\,\triangle t_i\right]_j ;\\
&where\ K_{wear-coefficient}\ is\ an\ adimensional\ and\ K,\\
&is\ the\ wear\ coefficient;\ N\ is\ cycle\ number\ ;\\
&The\ K_{wear-coefficient}\ is\ function\ of\ cross-shear\ ratio, CS,\\
&CS = \frac{E_{cross-shear}}{E_{total}}\ ,(adimensional)\ ;\\
&where,\\
&E_{cross-shear}\ :\ frictional\ work\ perpendicular\ component;\\
&E_{total}\ :\ total\ frictional\ work\ ;\\
&thus,\\
&K_{wear-coefficient} = [a+b+CS]^{\left(\frac{-1}{c}\right)}\ ;\\
&where,\\
&a,b,c\ :\ experimental\ constants\ ;\\
&CS\ :\ cross-shear\ ratio\ ;
\end{aligned}
\tag{2}
$$

[Casesnoves Bioengineering Laboratory. Algorithm-development-312]

Where, (in general from [7.1]),

Lwear : Linear abrasive wear (mm). It is set for both models.

Kwear- Coefficient: Wear Coefficient, standard (adimensional).

CS: Cross-shear ration. (adimensional), [7.1].

Ecross-shear: frictional work perpendicular component (work units).

Etotal: frictional work perpendicular component (work units). That is, sum (perpendicular+paralell components.

a,b,c: Experimental constants (adimensional, [7.1].

p_i : Pressure (N / mm^2).

v_i : Sliding discrete Velocity for discrete time increment (mm / s).

Δt_i : Discrete time interval (s).

i, j: Summatory indexes. The [**i**] is for velocity variation within a cycle (n). The [**j**] is for cycles number (N).

Just to remark, that the Kwear-Cross-Shear-Model and CS formulations set in Equation 2, can vary in the literature according to different authors [7.1-7.7]. However, what is a common finding is that the erosion magnitude predictions for UHMWPE TKA are higher for the cross-shear model than the classical Archard's one [7.1]. Dataset is implemented in intervals, Table 1.

CROSS-SHEAR MODEL SOFTWARE DATASET IMPLEMENTATION			
Parameter	**Magnitude Interval**	**Units**	**References**
Wear Coefficient	[1.36e-9, 5.50e-9] (exp-10 magnitude order)	adimensional	[7.1,7.3] Note that CSM is second generation and intervals vary
Wear Coefficient Constants, a,b,c	a= 8:5173 exp-65 ; b= 9:3652 exp-60 ; c= -6.7454 ;	adimensional note that c is negative	[7.1, 7.3]
Cross-Shear Ratio	[0 , 0.25]	adimensional	[7.1]
Sliding Distance	[40 , 80]	mm	[7.1]
Contact Area for linear wear calculations in Archard's models	[200 , 400]	mm2	[7.4] Note:at maximum flexion could reach 800 mm2, but extreme positions are not considered.

Table 1: Software implemented dataset for simulation-optimization of cross-shear model.

4. CROSS-SHEAR MODEL RESULTS

Figures 2-4 show the CSM linear wear for 1Mc, GNU-Octave imaging-processing system. Erosion magnitude is higher than Archard's model.

4.1 CSM GRAPHICAL OPTIMIZATION RESULTS

At Figure 2, the CSM linear wear for 1Mc, Matlab imaging-processing system. Erosion magnitude is higher than Archard's model. At Figures 2.1-4, the CSM linear wear for [1,5] Mc, Sliding distance in CSM is usually higher that Archard's model.

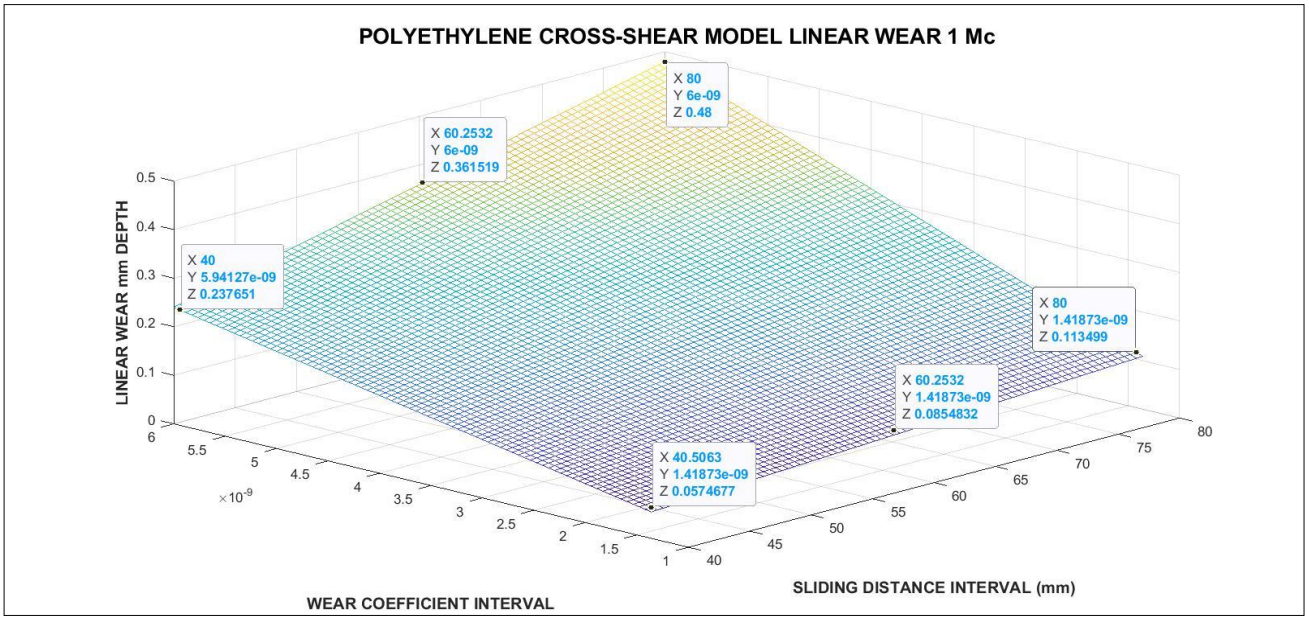

Figure 2: 1 Mc Matlab-2021 simulation of PE cross-shear model according to dataset of [7.1-7.4]. These cursor numerical results are used to make the Table 2. [Casesnoves Bioengineering Laboratory Software 2025-M-0].

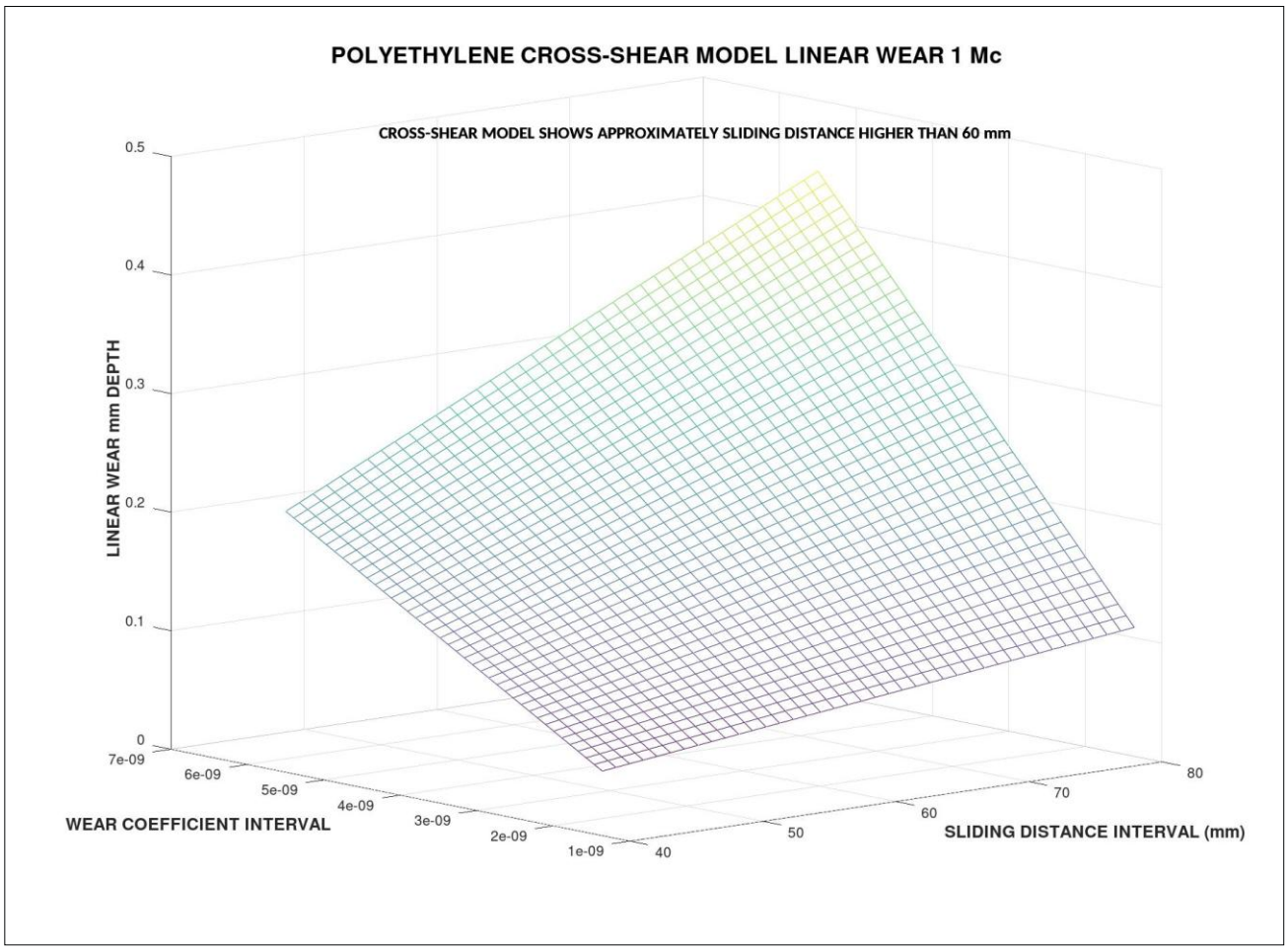

Figure 2.1: GNU-Octave simulation of PE cross-shear model according to dataset of [7.1-7.4]. [Casesnoves Bioengineering Laboratory Software 2025-M-1]. Image quality is not so perfect than Matlab but is acceptable.

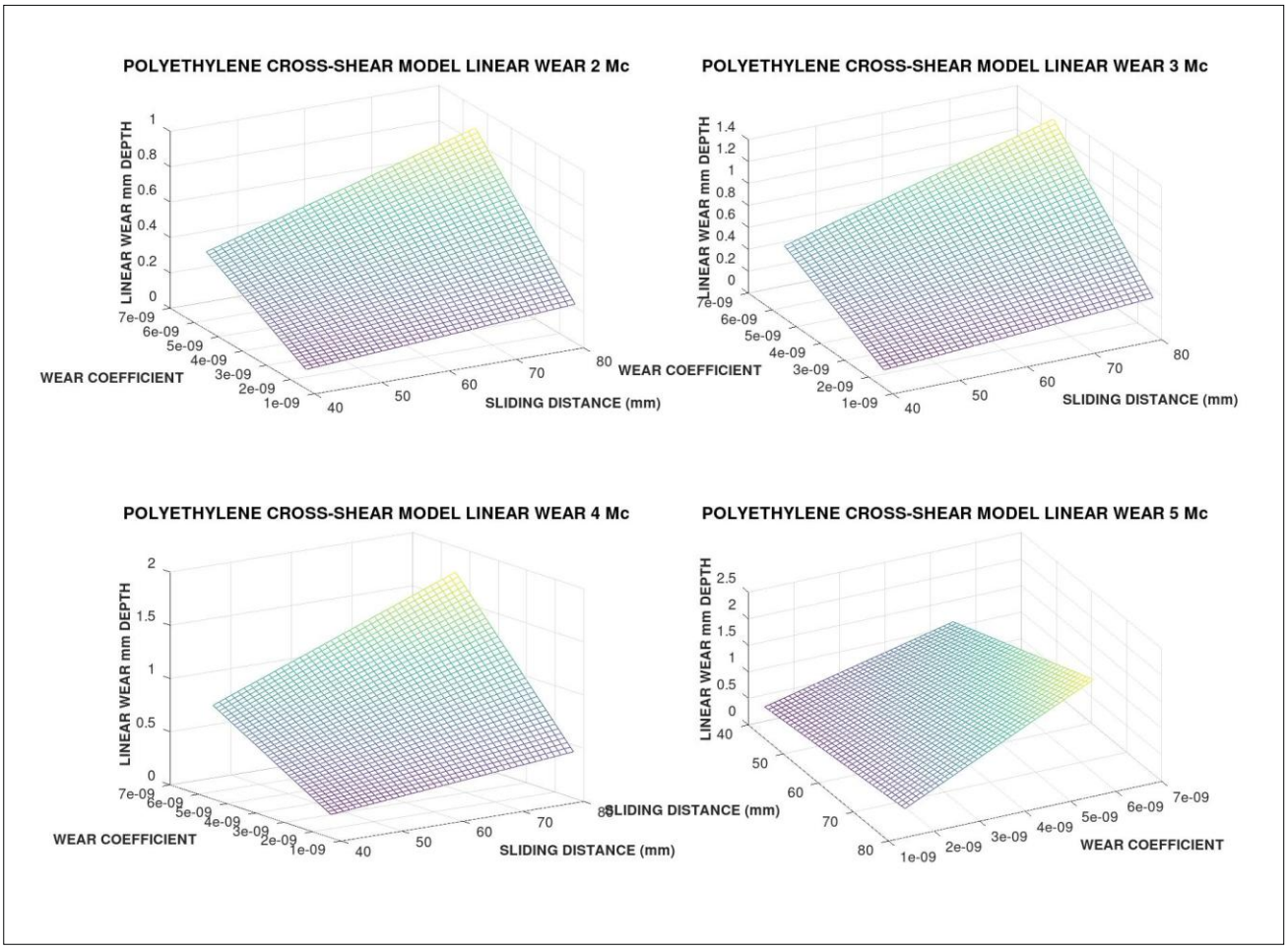

Figure 3: (2-5 Mc) GNU-Octave multisimulation of PE cross-shear model according to dataset of [7.1-7.4]. [Casesnoves Bioengineering Laboratory Software 2025-M-2].

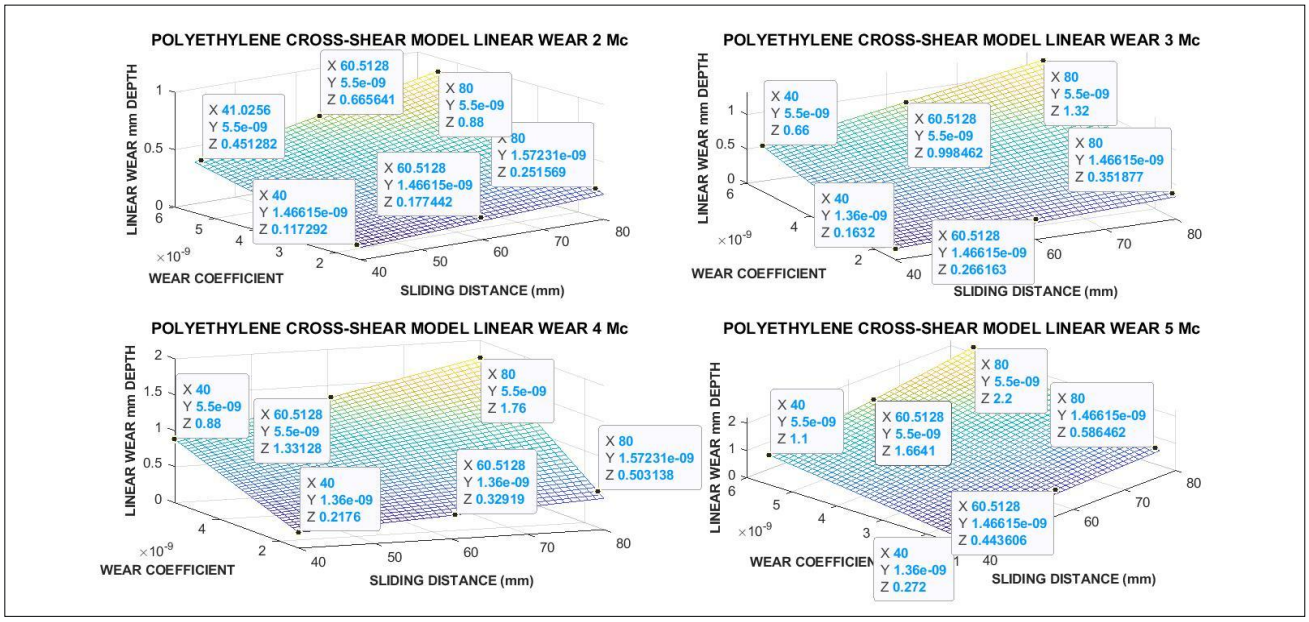

Figure 4: (2-5 Mc) Matlab multisimulation of PE cross-shear model according to dataset of [7.1-7.4]. [Casesnoves Bioengineering Laboratory Software 2025-M-2]. These numerical magnitudes are set in Table 2.

4.2 CSM NUMERICAL OPTIMIZATION RESULTS

Table 2 show the main numerical results for CSM with sliding distance intervals. Results are presented in closed max-min intervals, dividing the sliding distance in two intervals. Namely [40,60] mm and [60,80] mm. These cursor numerical results are used to make the Table 2.

CSM BRIEFING NUMERICAL RESULTS						
Mc	MIN (mm)	MAX (mm)	SLIDING DISTANCE INTERVAL (mm)	MIN (mm)	MAX (mm)	SLIDING DISTANCE INTERVAL (mm)
1	[0.06,0.09]	[0.24,0.36]	[40,60]	[0.09,0.09]	[0.36,0.12]	[60,80]
2	[0.12,0.18]	[0.45,0.67]	[40,60]	[0.18,0.25]	[0.67,0.88]	[60,80]
3	[0.16,0.27]	[0.66,1.00]	[40,60]	[0.27,0.35]	[1.00,1.32]	[60,80]
4	[0.22,0.33]	[0.88,1.33]	[40,60]	[0.33,0.50]	[1.33,1.76]	[60,80]
5	[0.27,0.44]	[1.10,1.66]	[40,60]	[0.44,0.59]	[1.66,2.20]	[60,80]

Table 2: Results of Graphical Optimization and simulations for CSM. Software implemented dataset for simulation-optimization of cross-shear model at Table 1. It is clear that CSM gives higher wear magnitudes than AM.

5. ARCHARD MODEL IMPROVEMENTS WITH REVIEW FOR TKA BIOMECHANICS

Before getting simulation-optimizations between cross-shear models and Archard's one, some TKA and knee biomechanical precision/concepts can be set. The biomechanics of TKA is rather complicated by a number of unlimited reasons, Figures, 1, 1.1 First, its most important function is the total weight support as the third biomechanical system of the anatomy, (first system in head-neck, second is thorax-abdomen-spine-hip, and third is knee-feet). That is, the legs and the feet. The second reason is the biodynamics of walk and movement that requires, while walking and moving, balance and support for the weight/gravity center of the total body. The third, and not the less, is that the articulations of knee, ankle, and feet constitute an essential biomechanical system for walk and basic life movements, [7.5]. Complementary reasons are the biomedical cartilage and bone aging-degeneration and forced movements injuries probabilities. All of them are mutually synergic and constitute an interrelated biomechanical system. In other words, if the knee joint cartilage degenerates soon, causes a bone damage, this creates instability and balance loss at knee, and in consequence the movement dynamics is limited or impeded. Just remind that histologically cartilage cells cannot regenerate like the elastic skin fibers (up to current science-research, it is tried to resolve the problem with stem cells, but that matter is out of this research scope). That is, any individual is born to get a fixed number of skin-organs elastic fibers and cartilage cells when his growth-development is completed. Furthermore, the second biomechanical system, in particular the hip articulation, can be damaged by forced/biased movements and biomechanical abnormal load distributions at knee joint. All this briefing gives a basic idea of the complications that may occur in surgical pathology and biomechanical diseases at knee articulation.

On the other hand and also, knee injuries, joint traumatological pathologies, and concomitant reumathological or infection diseases, creates a high medical-industrial demand. Then, the economic cost is rather high for both public, private, or mixed health services at many countries. Therefore, TKA investigation for reliability and high-durability of new TKA prostheses is among the current priorities in biomedical industry. Biomathematical studies with optimization modelling take the task for wear prediction and durability of TKA prostheses. An additional question is the number of model variants and large amount of different testing laboratories. This implies the requirement for standards methods

both experimental and theoretical-modelling. In this contribution, the most usual standards, ISO-related, [7.1-7.7], are prioritized for the objectives of this section of the study.

For comparison to cross-shear models, the mathematical equations and models used are for Linear Abrasive Wear (in mm) without Creep and Lubrication Factors [4] at this stage. For Volume Wear (in mm^3), the Finite Elements Method is widely applied in both models [8.1-8.11].

In summary, after these fundamental concepts introduction, this section of the study is focused on Archard's biomechanical model computational intelligence-optimization and new/review practical numerical and image processing results for mainly ultra high molecular weight weight polyethylene (UHMWPE) for this model. It is intended set sharp contrast with cross-shear models.

5.1 The Biomechanical Concepts of Knee Articulation

At Figures 1, 1.1, it is shown the basic knee biomechanical system after TKA implantation (parts and movement concepts). For normal life, the knee articulation supports biomaterials stress, loads, flexions, extensions, torsions, rotations and more complicated movements. Furthermore, it is not exclusively the articulation, ligaments, e. g., cruciate ones, and external, internal, lateral ligaments form a rather complicated articulated biosystem. This makes the incidence/prevalence of knee biomechanical pathology rather frequent. The sport activity increases these risks of injuries, and in that field, the knee articulation supports loads and extreme movements continuously. The sport-medicine specialization for knee is a branch with deep knowledge and applications.

5.2 Biomechanical Knee Implants

The most common TKA prostheses resemble the femur natural condyles, that is, they are bicompartmental. However, monocompartmental TKA prostheses have also been developed. Other type strand is TKA with fixed-bearing, and TKA with rotating bearing, [7.7]. For the standard TKA, the number of variants, related to biomaterials, biomechanical design, and forces-distribution designs are rather high. This makes complicated the laboratory testing, both *in vitro* and *in vivo*. What is more, the wear, creep, lubrication and other biomechanical parameters differ substantially in literature for the amount of methods, techniques, and laboratory apparatus, ISO variants are large, [7.6]. All in all, the TKA study constitutes a difficult biomechanical and biopathological field actually.

6. ARCHARD MODEL ALGORITHMS AND METHOD

Primary approximations are to consider exclusively the TKA wear, and exclude Creep and Lubrication Factors, (algorithms 3-6). Therefore, the calculations of this study part constitute the improvements/review of linear wear optimization-determination to get wear durability predictions of the TKA implant with fundamental physical formulation [7.5]. In the literature, variations of smodels are applied, e.g. [8.1, 8.4-8.6], although the most applied is Archard's model with several variants. Basic measurements taken into account in this study section for in vitro and in vivo and contact area correspond to [8.1-8.21]. Typical values of TKA wear, most times obtained by FE method are referred at [8.18-8.32]. It is not considered at present Archard's Volume Wear, e.g. [8.20], for this study.

6.1 The basic Model algorithm(s)

The basic algorithm-model from [8.3,8.11], applied and analyzed mathematically by Author, reads,

$$\textit{The Archard's Model applied on TKA,}$$

$$L_{wear} = K_{wear} \sum_{j=1}^{N} \left[\sum_{i=1}^{n} p_i \, |\overrightarrow{v_i}| \, \triangle t_i \right]_j ; \qquad (3)$$

Where,

L_{wear} : Linear abrasive wear (mm).

K_{wear} : Wear constant, standard (mm^3 / N mm). Note: at figures values range of K_w are usually multiplied by 10^{-3}.

p_i : Pressure (N / mm^2).

v_i : Sliding discrete Velocity for discrete time increment (mm / s).

Δt_i : Discrete time interval (s).

i, j : Summatory indexes. The [**i**] is for velocity variation within a cycle (n). The [**j**] is for cycles number (N).

6.2 The Creep and Friction Factors

Creep

Although those factors are not applied in the study, description with details of the Creep and Lubrication formulas are conveniently shown. Creep equations are usually very similar for both models, Archard's and Cross-Shear. For Creep, [8.3], the Archard's model-equation format (Lee and Pienkowski, 1998) reads.

The Archard's Model complemented with Creep, applied on TKA,

$$L_{total\ wear} = L_{linear\ wear} + L_{creep};$$

Hence,

$$L_{total\ wear} = L_{linear\ wear}\ [K_1 + K_2\ (\log t - 4)]\ P_{average}\ h; \quad (4)$$

Where,

K_1: Model Constant, [3]. Values for K_1 and K_2 are respectively, 3.491×10^{-3} and 7.961×10^{-4}.

K_2: Model Constant, [3]. Values for K_1 and K_2 are respectively, 3.491×10^{-3} and 7.961×10^{-4}.

t: Time of load (minutes).

$P_{average}$: (N/mm^2)

h: Polyethylene thickness (mm)

6.3 Friction

One common Friction Factor, set within the general formula is: [$1+3\ \mu^2$]^{½} , [21], with values for UHWMPE of around [10^{-2}] magnitude order. This Friction factor multiplies linearly the general formula (1). At this stage, it is not applied in the study. Friction was not set at this stage because the friction value in this case is, approximately.

(1+3 x 0.072) $^{0.5}$ = 1.0073, [adimensional] (5)

That is, a magnitude order of 10^{-3}. This implies that the magnitude difference if set within algorithms would not determine a magnitude order significance. That precision is useful for further refinements.

6.4 The Integral AM Algorithm

It is convenient, when experimental data or database available, to compute the algorithm in integral-equation of first kind. Hence, taking trivial derivatives, integral, and limits for getting an integral form.

The Archard's Model applied on TKA, integral form,

$$L_{wear} = K_{wear} \sum_{j=1}^{N} \sum_{i=1}^{M} \left[\int_0^{t_i} p\, |\vec{v}|\, dt \right]_j \quad ; \quad (6)$$

Where,

L_{wear} : Linear abrasive wear (mm).

K_{wear} : Wear constant, for programs (mm^3 / N mm) . Note: at figures values range of K_w are usually multiplied by 10^{-3} because of this change of units (generally K_{wear} is formulated (mm^3 / N x m).

p(t) : Instantaneous pressure (N / mm^2). Function of time.

v(t) : Instantaneous sliding velocity for integral. Function of time (mm / s).

dt : Differential of time during i-interval (s).

i ; Summatory index for time at every integral for a cycle (M).

j ; Summatory index for total cycles (N).

Proof

$$
\begin{gathered}
The\ Archard's\ Model\ applied\ on\ TKA,\ integral\ form\ proof, \\
For\ one\ cycle, \\
L_{w1} = K_w p S; \\
where\ S\ is\ sliding\ distance,\ hence \\
L_{w1} = K_w p\, v\, t; \\
therefore, provided\ \vec{v}\ constant\ and\ taking\ derivatives\ for\ time\ variable\ , \\
\tfrac{dL_{w1}}{dt} = K_w p\, v\ ;\ or, \\
dL_{w1} = K_w p\, v\, dt,\ integrating, \\
\textstyle\int_0^t dL_{w1} = \\
K_w \textstyle\int_0^t p\, v\, dt,\ supposing\ instantaneous\ pressure\ and\ sliding\ velocity\ during\ one\ cycle\ , \\
Therefore, taking\ N\ cycles,\ and\ integrating,
\end{gathered}
\tag{7}
$$

$$
L_{wear} = K_{wear} \sum_{j=1}^{N} \sum_{i=1}^{M} \left[\int_0^{t_i} p\, |\vec{v}|\, dt \right]_j ;
$$

[Algorithm developed by Casesnoves Bioengineering Laboratory Algorithm 3114]

6.5 Computational Intelligence Dataset Software

Dataset, Tables 3-4, selected from literature is selected from wide ranges at programs, because the commercial materials, TKA sizes, and Algorithm constants applied differ among authors, laboratories, testing apparatus, testing temperature, etc. As a result, it is necessary to choose those experimental datasets/magnitude-values which are commonly accepted in the literature. Therefore, the practical objective of the simulation-optimizations is to provide with large scale range that can be used to predict durability for all of those most important variants. Software is based on hip wear previous Author's contributions for hip wear programming design [9.33-9.34]. In those publications, both Tikhonov Regularization Theory and Evolutionary Algorithms were applied for hip optimization software-engineering. General additional biotribology database can be found at [9.35-9.45].

6.5.1 Average Contact surface Magnitude

That is a parameter interval rather difficult to implement within programs, both in Matlab and GNU-Octave. For both models in this study, the intervals published in [7.4] are set. Tables 3-4.

6.5.2 Benchmark polyethylene model

Continuing with previous subsection, there are variations for the TKA size in literature about laboratory studies. However, the size used for simulation software implementation was the most standard one, [7.1-7.3, 8.10]. That is, 78.2 x 44.2 mm the total coronal dimension, from that magnitude the contact surface was approximated-calculated. That size is according to ISO, and it is noteworthy to consider that there are ISO variants. Tables 3-4.

6.5.3 Sliding Distance (SD)

Sliding distance recommended by ISO is about 80 mm [8.10]. However, it was set [60,80] mm, taking into account differences between prostheses sizes, [8.12]. Tables 3-4.

6.5.4 Load Magnitude Interval

This is a magnitude convergence point for most of studies. The most usual assumed magnitude by majority of investigations [8.21, 8.21.1, 8.21.2]. For example [8.2, Table 2, page 63] gives an overview of the changes of loads and gaits from normal walk to down stairs/ramp. From this Table and setting a patient average weight of 75 kg, the interval

of loads that comprise approximately walk, stairs and clim down/up, etc, can be deducted. Usually, then, is [1600, 2600] N interval. Here it is taken a maximum of 2300-2600 N in most simulation-programs. Other Authors, [8.21], apply a maximum load of 3000 N. That is not considered for this study, because those loads are not for usual patient walk. That is, walk to down stairs in a normal patient activity happens during a few minutes in general. Tables 3-4.

6.5.5 Standard Unit System

The Linear Wear standard TKA erosion Archard's model units used in literature, most times, are mm^3 of eroded material or mm depth of erosion along contact surface. When studies are in vivo or provided with cadaveric history, the Linear Wear is given in mm/year. It is not an objective of this study to discuss the optimal unit system. Instead, the image-processing and numerical data is expressed in mm depth to bring for user the choice to compare dataset appropriately, [7.6,8.3,8.11]. The numerical comparative Table 6 shows AM approximations for the publications with mm/year. This is done taking into account the average Mc for a year, [8.16], which is about 2 Mc/year—precisely, that is a rather difficult parameter since variations among patient groups, countries, and laboratories are high. The physics dimension equations for AM Linear and Volume Abrasive Wear are explained in Equations (8). Tables 3-4.

6.5.6 Standard Abrasive Wear Factor K_w Magnitude

Given the fact that the number of laboratory apparatus, measuring systems, and hybrid studies are profuse, in the literature, there is not a total agreement for K_w magnitude [8.3]. Figures 5-6 show 2D GNU-Octave imaging processing multi-polynomial fit that describes the variation in function of K_w variation and Million Cycles [8.13-8.21] integer interval. Note: at figures values range of K_w are usually multiplied by 10^{-3}. Figure 5 shows AM linear wear related to Load-Mc parameters. Figure 6 presents AM linear wear related to wear factor K_w from 1 -5 Mc Tables 3-4.

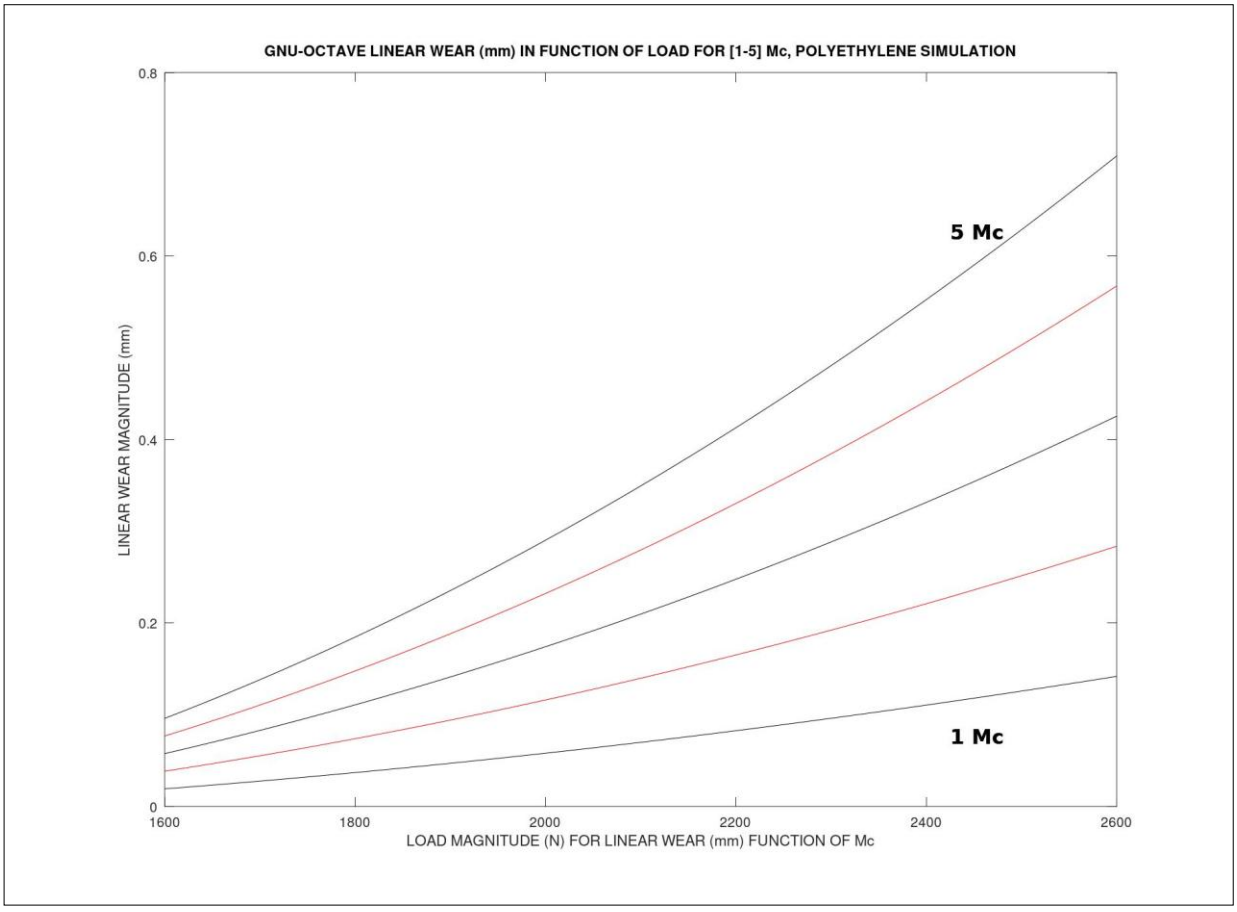

Figure 5: For parameters of Tables 3-4, example of polynomial fit for wear prediction in function of the load variation range of [1600,2600], (continuous), and Mc [1,5] (integer). It is clear the wear magnitude variation related to increase of load and the Mc number. Note: at figures values range of K_w are usually multiplied by 10^{-3}. Previously the 2D imaging processing, a 3-degree polynomial fit was developed for every million-cycle graph-line type. This type of software is developed from Author's series of previous publications in hip prostheses wear and other computational contributions [7.5,9.33-9.34]. [Casesnoves Bioengineering Laboratory Software 2025-M-3].

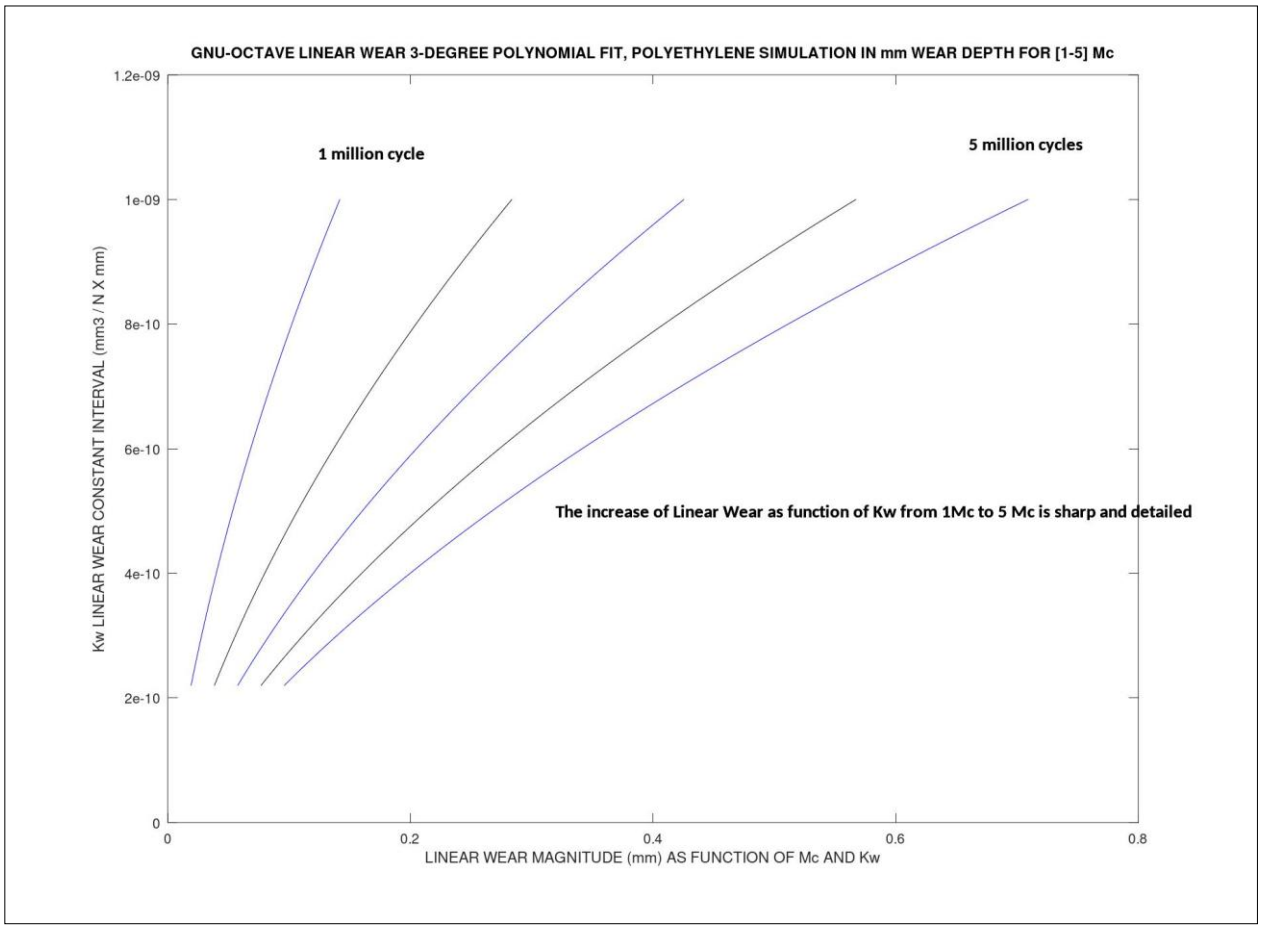

Figure 6: For parameters of Tables 3-4, example of polynomial fit for wear prediction in function of the variation range of [K_w x 10^{-3}], (continuous), and Mc [1,5] (integer). It is clear the magnitude variation related to increase of [K_w x 10^{-3}], and the Mc number. Note: at figures values range of K_w are usually multiplied by 10^{-3}. Previously the 2D imaging processing,a 3-degree polynomial fit was developed for every million-cycle graph-line type—different from precious Figure 5. This type of software is developed from Author's series of previous publications in hip prostheses wear and other computational contributions [7.5,9.33-9.34]. [Casesnoves Bioengineering Laboratory Software 2025-M-4].

6.5.7 AM Units Precision

Equation 8 shows the physics units system implemented for AM simulations. The same units were used for CSM, that is N, mm, and mm2. Also, Tables 3-4.

$$\textit{Standard literature units for Archard's model dimension equations, For example,}$$

Erosion in mm depth,

$$L_w\,(mm\,depth) = K_w\,(\tfrac{mm^3}{N\,mm})\,Pressure\,(\tfrac{N}{mm^2})\,Sliding\,Distance\,(mm); \quad (8)$$
$$as\,a\,result\,, L_w\,is\,in\,mm,$$

Erosion in mm^3 eroded material volume,

$$V_w\,(mm^3 volume) = K_w(\tfrac{mm^3}{N\,mm})\,PressureForce(\,N\,)Sliding\,Distance(mm);$$
$$as\,a\,result\,, V_w\,is\,in\,mm^3;$$

For AM, the first one is the primary method applied in this paper. That is Abrasive Linear Wear. Volumetric knee-biotribology wear will be developed in further studies.

SELECTED STANDARD DATASET USED FOR COMPUTATIONAL SIMULATIONS			
PARAMETERS AND UNITS	**INTERVAL OR MAGNITUDE SOFTWARE IMPLEMENTED**	**REFERENCES**	**PRECISION**
LOAD (N)	[1600-2000,2300-2600] Generally, [2000,26000]	[7.1,7.5,8.1,8.11,8.21,8.21.1,8.21.2]	Standard magnitude, usually agreed by most authors. The most implemented interval was [2000,2600] .
SLIDING DISTANCE (mm)	[60,80]	[8.10]	ISO Standard, it varies according to studies. Usually was implemented 60 mm.
WEAR FACTOR **K_w (mm^3 / (N x mm)** **[Note, it is wear factor for AM, not wear coefficient for CSM]**	[2.20×10^{-7} , 10^{-6}] [Note: at figures values range of K_w are usually multiplied by 10^{-3} because all the units are set in mm at software]	[8.3,8.21]	The wear factor constant K_w has different values in literature. It is implemented an interval that comprises most published magnitudes.
LOAD SURFACE **(mm^2)**	[200 , 800]	[8.21, 8.21.1,8.21.2]	This varies significantly according to several publications.
CYCLES NUMBER **(in M (millions) cycles)** **notation standard: Mc**	[1 , 5] image-processing is shown for [1 , 5] Mc	[8.1-8.11, 8.13-8.32]	It is presented, usually, in most books and papers dataset from 1 M to 5 M. Most authors show predictions and calculation testing for 1-5 Mc.
WEAR FACTOR IMPLEMENTED: **K_w (mm^3 / (N x mm)) x 10^{-3}** **according to (3)**	[2.20×10^{-10} , 10^{-9}] See Figures 1-8	[8.3]	K_w has different magnitude according to authors, [8.3], and some researchers propose values of K_w , for example [8.21] .
Poisson ratio and Elastic modulus, Density, for UHMWPE	**NOT IMPLEMENTED,** **EXCLUSIVELY ILLUSTRATIVE** **UHWMPE: Young's modulus 463 MPa, Poisson' ratio 0.46, density 960 kg/m^3 [21.1].**	[8.21]	N/A for the algorithms which are programmed.

Table 3: Selected Dataset used for simulations and optimization software. Disclaimer: some variants were applied for trial programs and images. Note 1: at figures many times values axe-range of Kw are multiplied by 10-3. Note 2: inconsistency at 'generally [2000,26000], it should be [2000,2600] at Load (N) row.

AM SOFTWARE-ENGINEERING PARAMETER-INTERVALS LITERATURE REFERENCES		
PARAMETER AND UNITS	**REFERENCES FOR SOFTWARE IMPLEMENTED**	**EXTENSIONS**
LOAD (N)	[8.1,8.11,8.21,8.21.1,8.21.2]	Standard magnitude, usually agreed by most authors. It is important to set at patterns an magnitude interval as wider as possible to get trustful comparisons/predictions.
SLIDING DISTANCE (mm)	[8.10]	ISO Standard, it varies, from [40,80] mm usually. For CSM is generally longer.
Wear Factor K_w (mm^3 / (N x mm)	[8.3,8.21]	The, [8.3], range is applied for software. Recalling to note the difference between wear factor (AI), dimensional, and wear coefficient (CSM), dimensional.
LOAD SURFACE (mm^2)	[8.21, 8.21.1,8.21.2]	[8.1] shows standard coronal size and loads.
CYCLES NUMBER (in M (millions)) notation standard: Mc	[8.1-8.11, 8.13-8.32]	It is presented, usually, dataset from 1 Mc to 5 Mc . In the literature, the most usual is show a range [1,5] Mc.
Wear Factor IMPLEMENTED: K_w (mm^3 / (N x mm)) x 10^{-3}	[8.3]	It is considered sufficient confident interval that comprises almost all authors publications.
Poisson ratio and Elastic modulus for UHMWPE	**NOT IMPLEMENTED,EXCLUSIVE ILLUSTRATIVE, UHWMPE: Young's modulus 463 MPa, Poisson ratio 0.46, density 960 kg/m^3 [8.21].**	N/A for the algorithms which are programmed.

Table 4: Selected Dataset used for simulations and optimization software. Disclaimer: some variants were applied for trial programs and images. Note: at figures many times values axe-range of K_w are multiplied by 10^{-3}.

6.6 Computational intelligence Software

The most important parts of the software are mainly two. Both are difficult. The first one is the matrices setting withing patterns and their congruence for mathematical operations. The second hurdle is the 2D-3D imaging processing subroutines setting, because not any order for getting an accurate image is efficacious when obtaining the 2D-3D image.

6.6.1 Differences Between AM and CSM implementation Algorithms

There are specific important differences when implementing the CSM and AM models in software patterns. These are,

1. CSM model is linear, easier to set, while AM model could be nonlinear, since contact surface is at denominator, dividing.
2. Therefore, when setting matrices for imaging-processing, CSM is simpler, and AM requires a careful matrix congruence calculation work.
3. Setting parameter intervals, therefore, is rather difficult in AM. On the contrary, for CSM model that task, although also complicated, is simpler.

6.6.2 Programming Structure

It was developed software programming mainly from previous experience in hip wear models [8.33,8.34]. Systems used were Matlab 2023 and GNU-Octave 8.1.0. For programming algorithms 1-2, the difficulty was the matrices congruency and the loops for arrays. Figure 3 shows the software pattern to check image-processing quality. Sketchs 1-2 explain the basic programming structure.

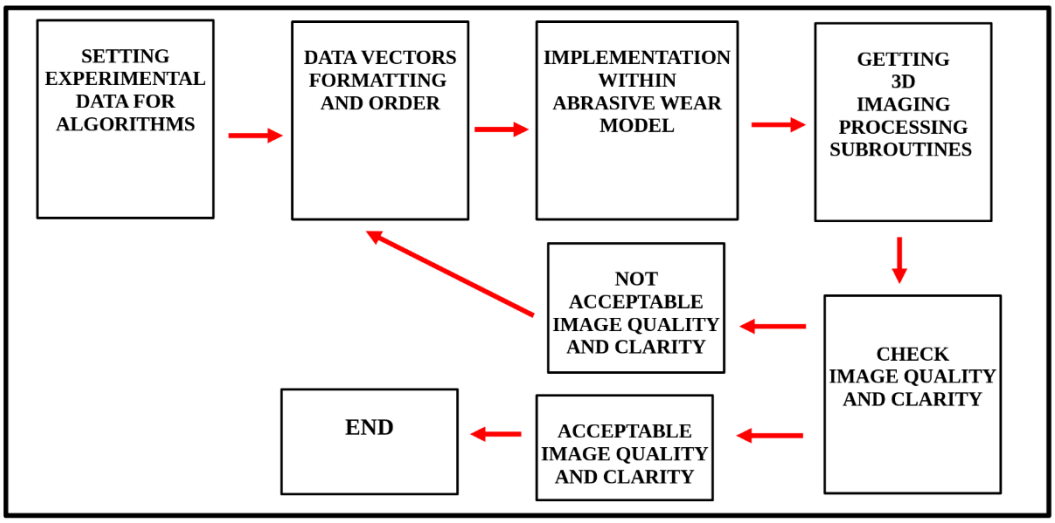

Sketch 1: Basic programming flow chart that shows the software pattern to check image-processing quality. The foremost essential is to gather trustful experimental data. Secondly important in those programs are the arrays and their implementation within the algorithm. The experimental dataset can be vectorized in many forms, and the selection of the optimal one is crucial. If the dataset-vectors are not conveniently re-arranged and set at the 3D imaging processing subroutines, the resulting image could not be acceptable. There are image-processing tools in Matlab and GNU-Octave to improve image clarity and sharpness. [Casesnoves Bioengineering Laboratory Software 2025-M-4]

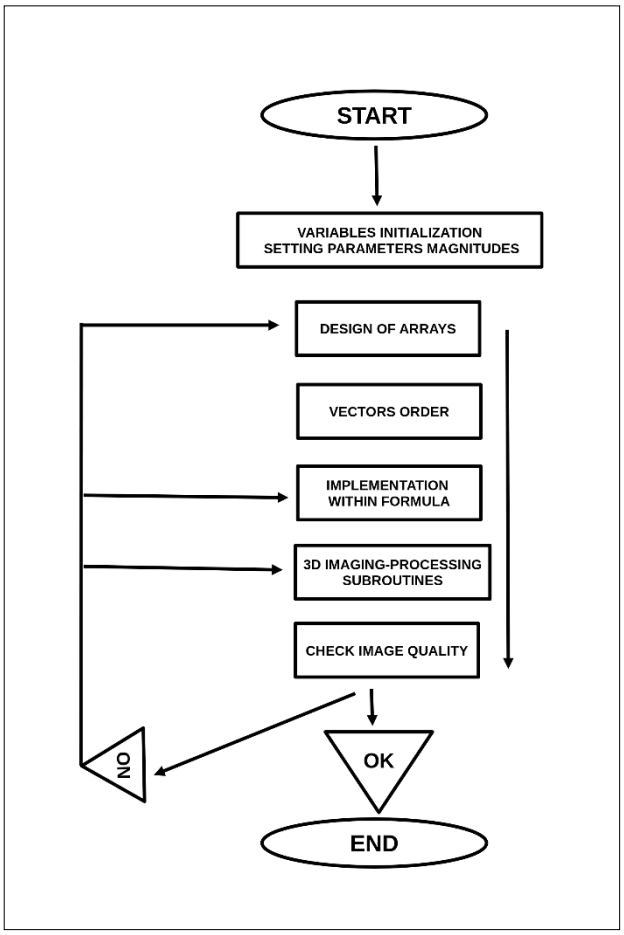

Sketch 2.-Complementary and basic programming flow chart. The most important of those programs are the arrays and their implementation within the algorithm. If the dataset-vectors are not conveniently re-arranged and set at the 3D imaging processing subroutines, the resulting image could not be acceptable. Note: at figures many times values axe-range of K_w are multiplied by 10^{-3}. This type of software is developed from Author's series of previous publications in hip prostheses wear and other computational contributions [9.33-9.34]. [Casesnoves Bioengineering Laboratory Software 2025-M-5].

7. AM RESULTS

Results are divided into Graphical and Numerical. In this primary stage, the numerical ones were determined by Matlab graphical methods. The sharpness of 3D Graphical optimization is acceptable, and numerical figures show approximate coincidence with standard literature, Table 5, [8.13-8.18]. Briefing of numerical comparisons to other Authors with Graphical Abstarct are detailed in Table 6.

Computational intelligence Software

The software programming was developed mainly from previous experience in hip wear models and knee articles, [7.5,9.33-9.34,9.45]. Systems used were Matlab and GNU-Octave. For programming algorithms 1-2, the difficulty was the matrices congruency and the loops for arrays.

7.1 Graphical Optimization Results

Graphical Optimization Method was developed during PhD Thesis and PhD Program publications, later in series of articles [7.5,9.33-9.34,9.45,9.56]. It essentialy consists in finding the global/local minima by searching along the implemented 2D-3D imaging surfaces/curves of the algorithm objective function plus one/two selected parameters. Here it is applied on the wear formulas (3,6,8) to determine the optimal minima or any desired values subject to particular constraints along the 3D surface. In Illustrative Example 1, it can be seen the process initiation. Firstly, some tentative programs are designed, after that, when checking the functionality of the software and the numerical congruence of the 3D graphs, the definite 3D Graphical Optimization Image-Processing charts are done with accurate parameters and intervals.

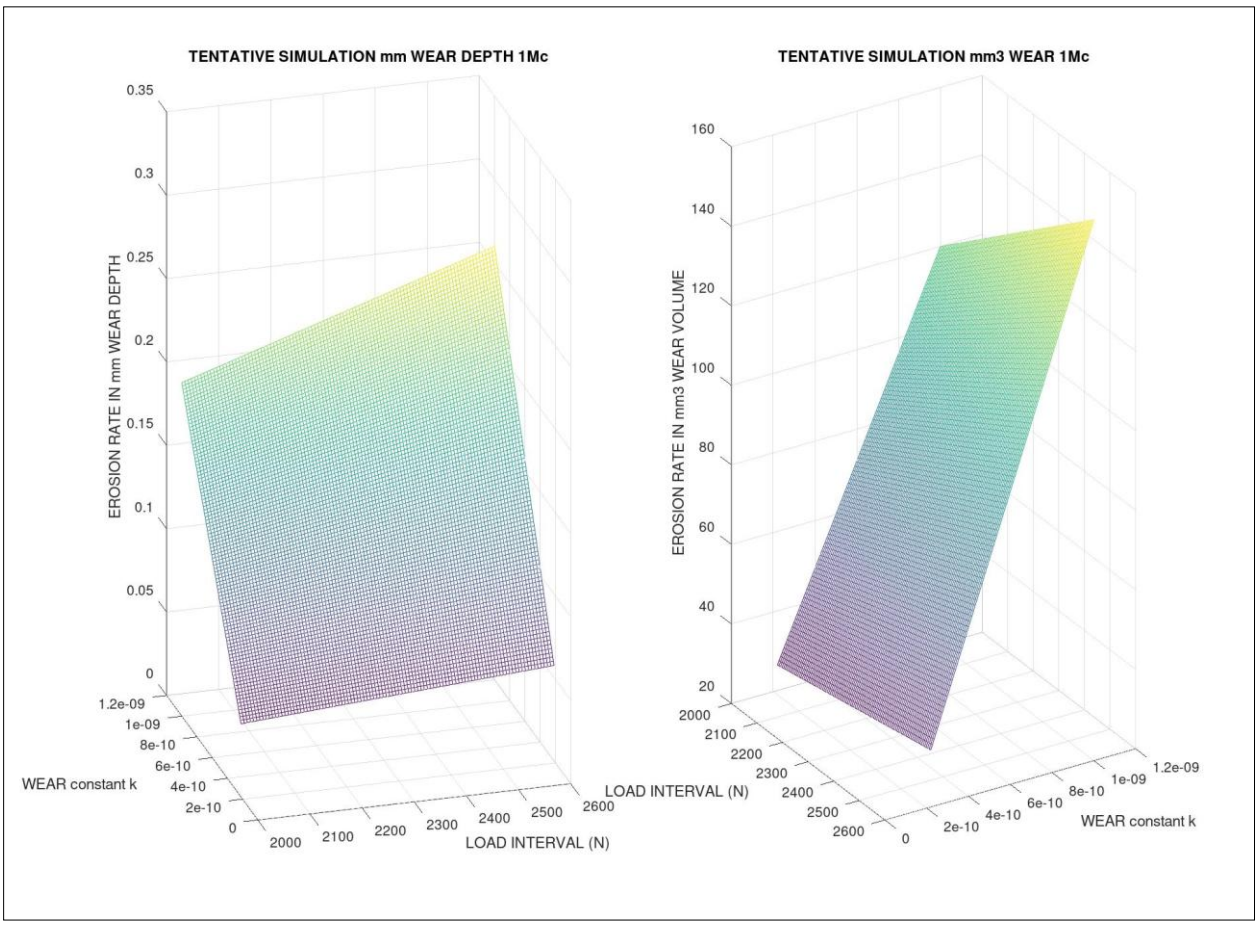

Illustrative Example 1: First trial tentative simulation with GNU-Octave. It is shown the basic model simulated in wear mm depth (when the surface contact is implemented), and (right), the basic model simulated in wear mm^3 volume. Since it is tentative to show the computational method, magnitude-parameters model is not too much significative. Matlab programs are equivalent. [Casesnoves Bioengineering Laboratory Software 2025-k-1] Volumetric wear is exclusive tentative, not the objective of the study, that program is got setting the volumetric algorithm formula at (8).

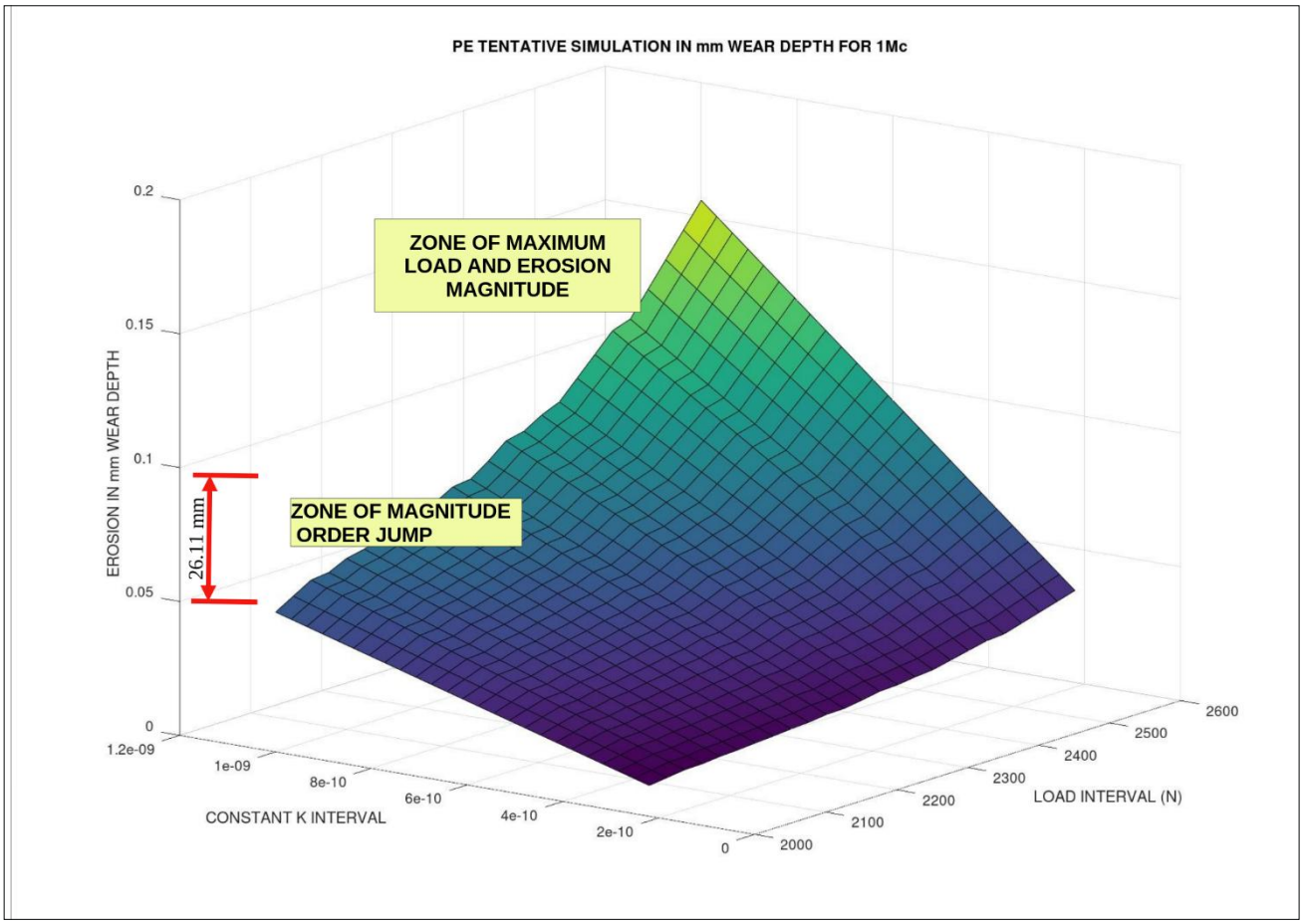

Illustrative Example 2.- Continuing the software improvements, second trial tentative simulation with GNU-Octave. It is shown the basic model simulated in wear mm Linear Depth (when the surface contact is implemented at denominator). It is set 1 Mc. Since it is tentative to show the computational method, magnitude-parameters model is not too definite, but approach experimental laboratory literature, [8.1-8.6]. Matlab programs are equivalent, but not exactly equal. [Casesnoves Bioengineering Laboratory Software 2025-k-2].

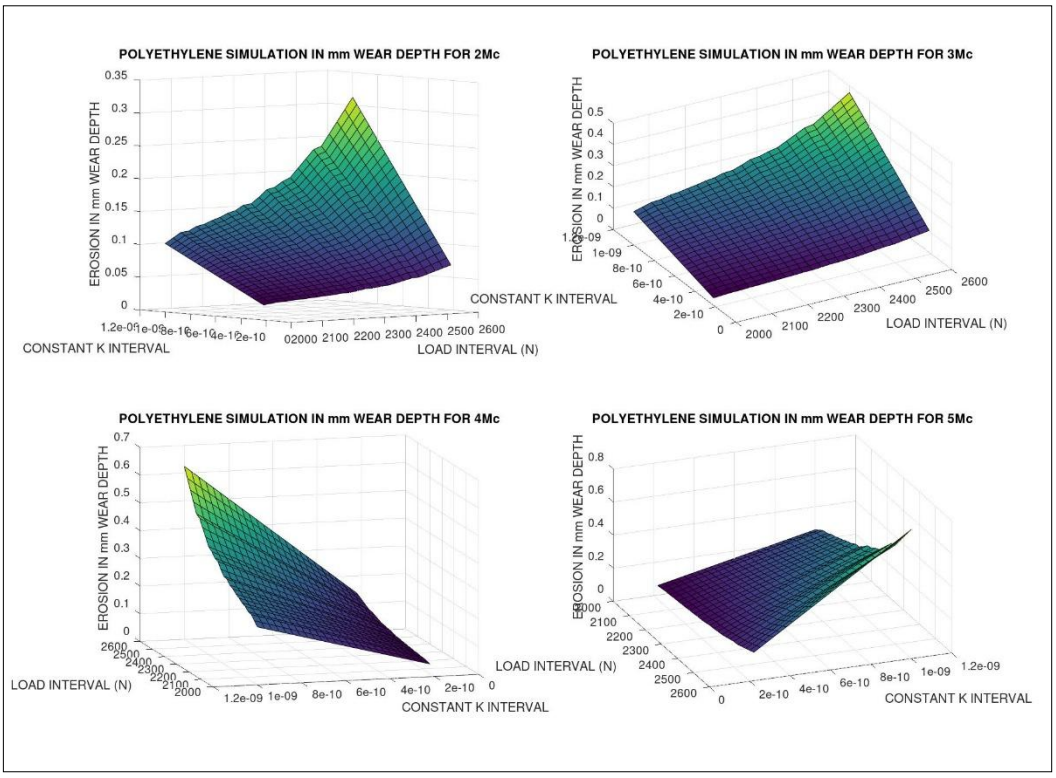

Figure 7: Selection of variables load and wear factor K at x-y plane. Multiple simulation with GNU-Octave for (2-5) Mc. It is shown the basic model simulated in wear mm depth (when the surface contact is implemented. It shows the different wear magnitudes when Mc are increasing. The computational method, magnitude-parameters belong to Table 3. GNU-Octave imaging-processing is acceptable. This figure software is also developed in Matlab, Figure 8. [Casesnoves Bioengineering Laboratory Software 2025-k-3].

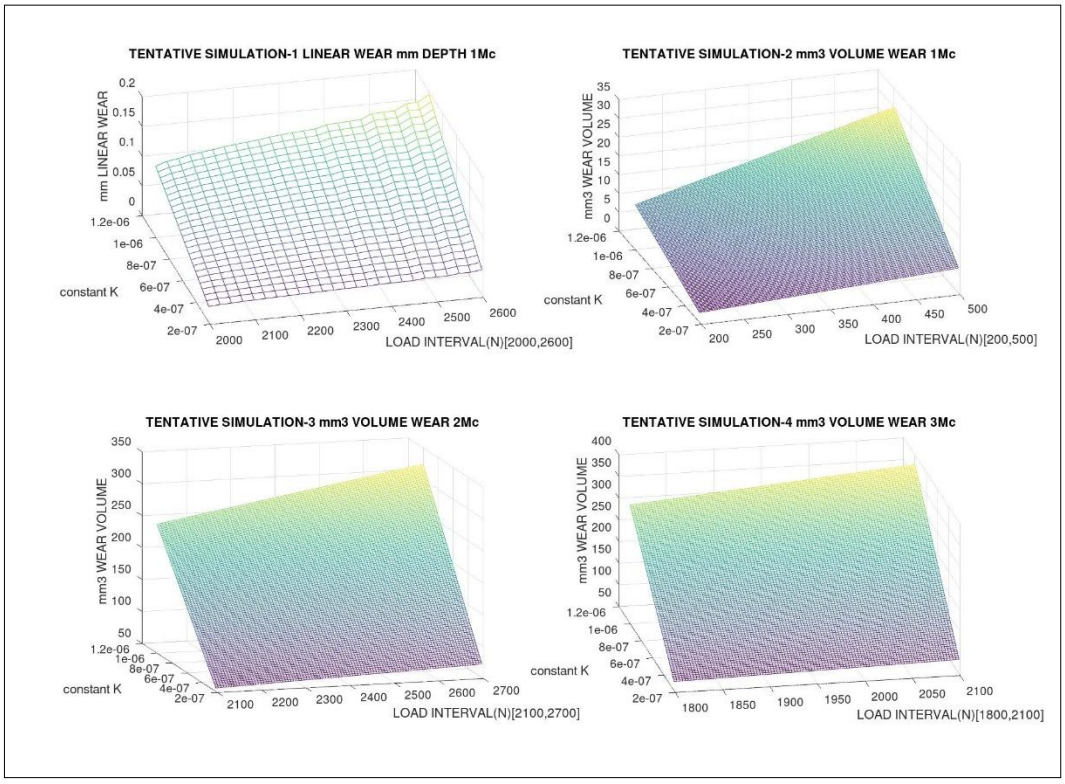

Figure 7.1: First trial tentative quadruple-simulation with GNU-Octave and two different 3D imaging processing subroutines (1-3) Mc. The intention is to check the different image qualities and the correct running of the programs. It is shown the basic model simulated in wear mm depth (when the surface contact is implemented), image 1, and the basic model simulated in wear mm^3 volume, images 2-4. Since it is tentative to show the computational method, magnitude-parameters model are not too much exact yet. However, it is clear the magnitude junp from 10exp(-2) to 10exp(-1)at image 1. Matlab programs are equivalent. [Casesnoves Bioengineering Laboratory Software 2025-k-1]. The loads are varied intervals, the K wear factor constant interval is approximately [10^{-6} , 10^{-7}] . Note: at figures, not precisely here, many times values axe-range of K_w are multiplied by 10^{-3}. [Casesnoves Bioengineering Laboratory Software 2025-M-6].

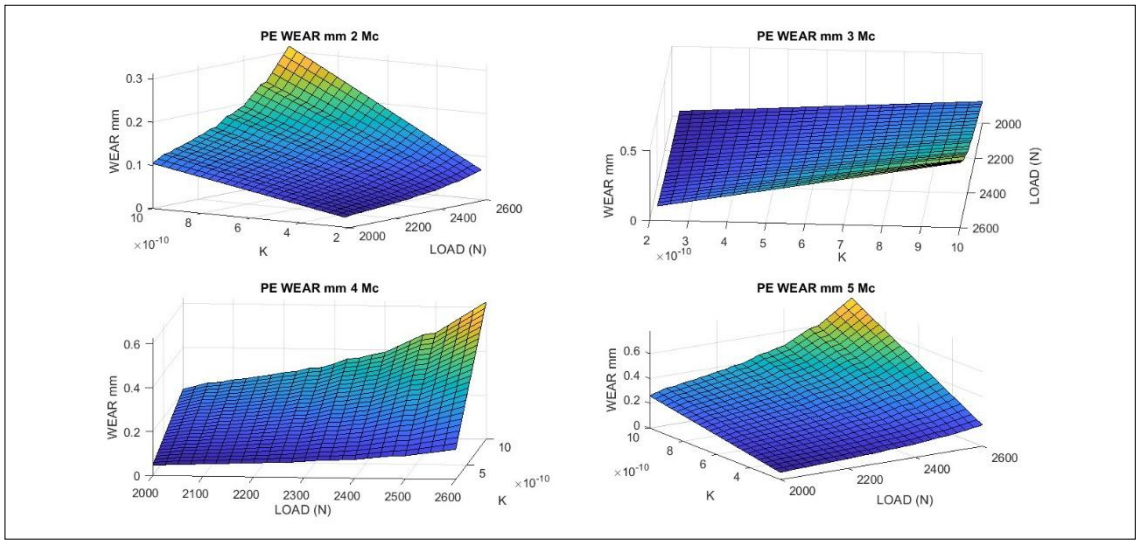

Figure 8: Multiple simulation with Matlab, (2-5 Mc). It is shown the basic model simulated in wear mm depth (when the surface area is implemented). It shows the different wear magnitudes when Mc are increasing. The computational method, magnitude-parameters belong to Sketchs 1-2, and Tables 3-4. Note the K wear factor constant magnitude orders. Matlab image-processing is better than GNU-Octave in this case. [Casesnoves Bioengineering Laboratory Software 2025-k-4].

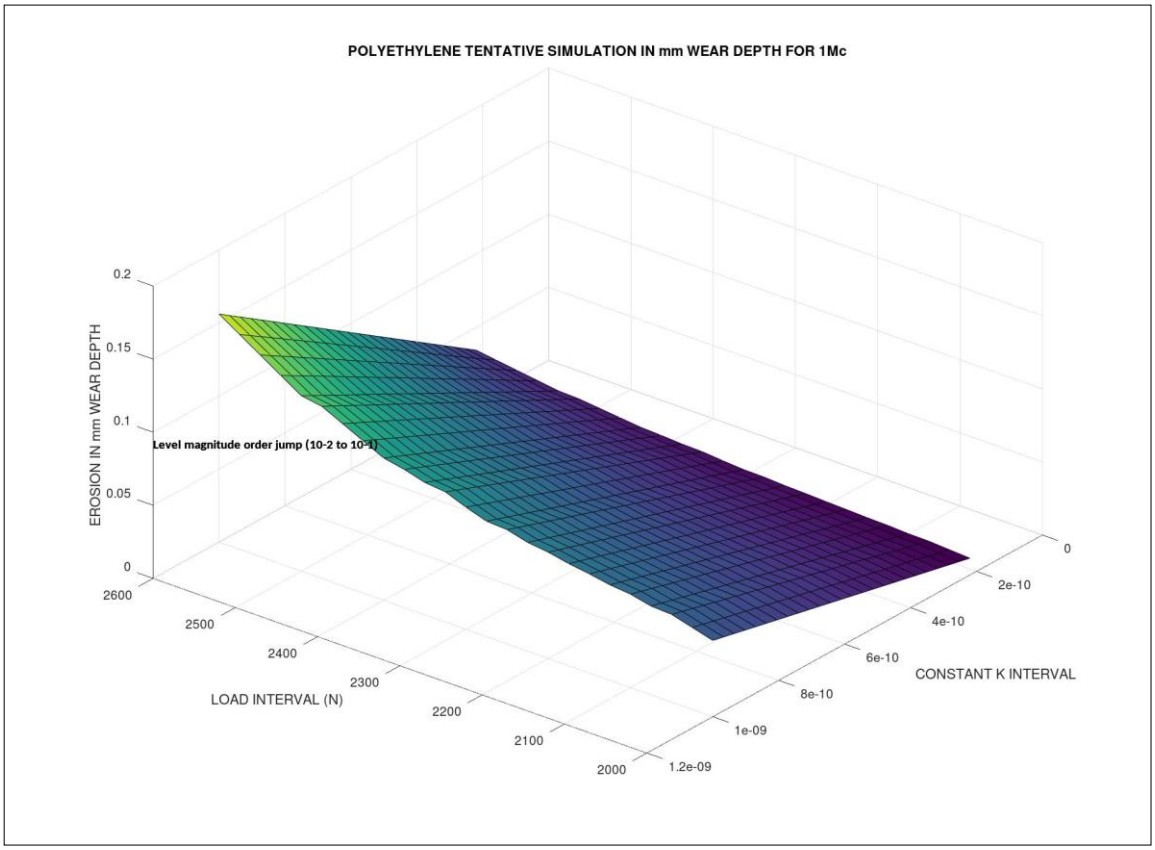

Figure 8.1: The purpose of this chart is to demonstrate the linear wear magnitude jump from 10(exp-2) to 10(exp-1), marked inset. It is shown the basic model simulated in wear mm linear depth (when the surface contact is implemented at denominator). Matlab programs are equivalent, and in general Matlab 2D-3D image quality is superior than GNU-Octave, [Casesnoves Bioengineering Laboratory Software 2025-k-2]. Note: at figures many times values axe-range of K_w are multiplied by 10^{-3}. [Casesnoves Bioengineering Laboratory Software 2025-M-7].

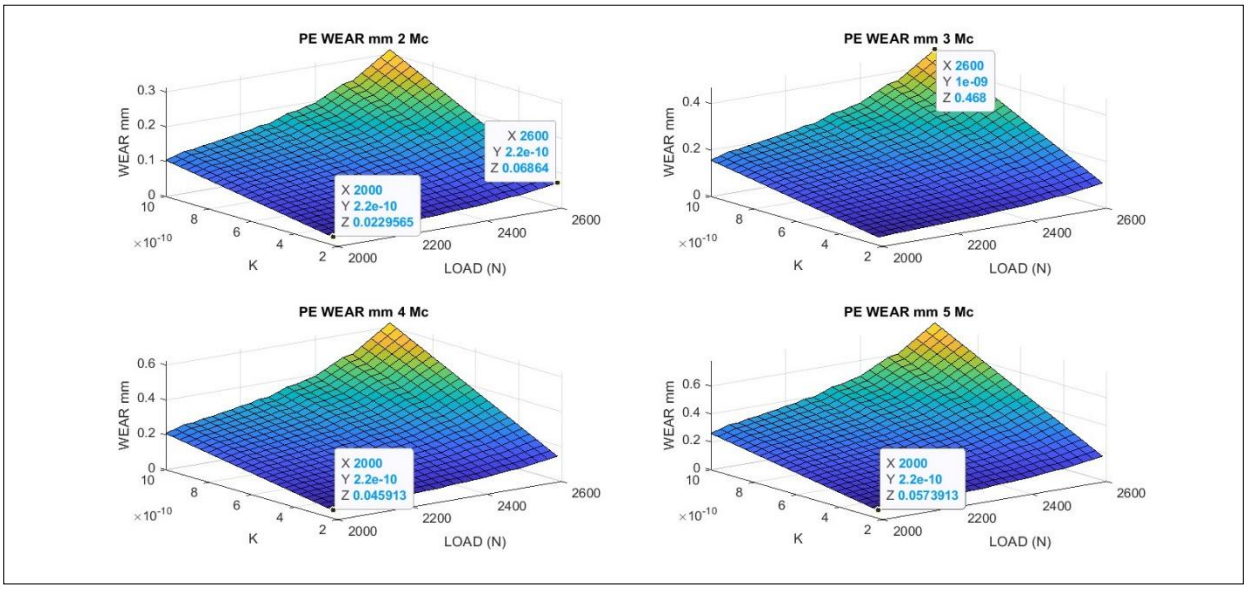

Figure 9: Note the cursor utility in Matlab to extract numerical data easily. From Figure 8, a number of dataset values implemented at image. That is, a number of graphical data for multiple simulation with Matlab, (2-5 Mc). It is shown the basic model simulated in wear mm Depth (When the surface area is implemented). It proves the different wear magnitudes when Mc are increasing. Matlab image-processing is better than GNU-Octave in this case. [Casesnoves Bioengineering Laboratory Software 2025-k-5].

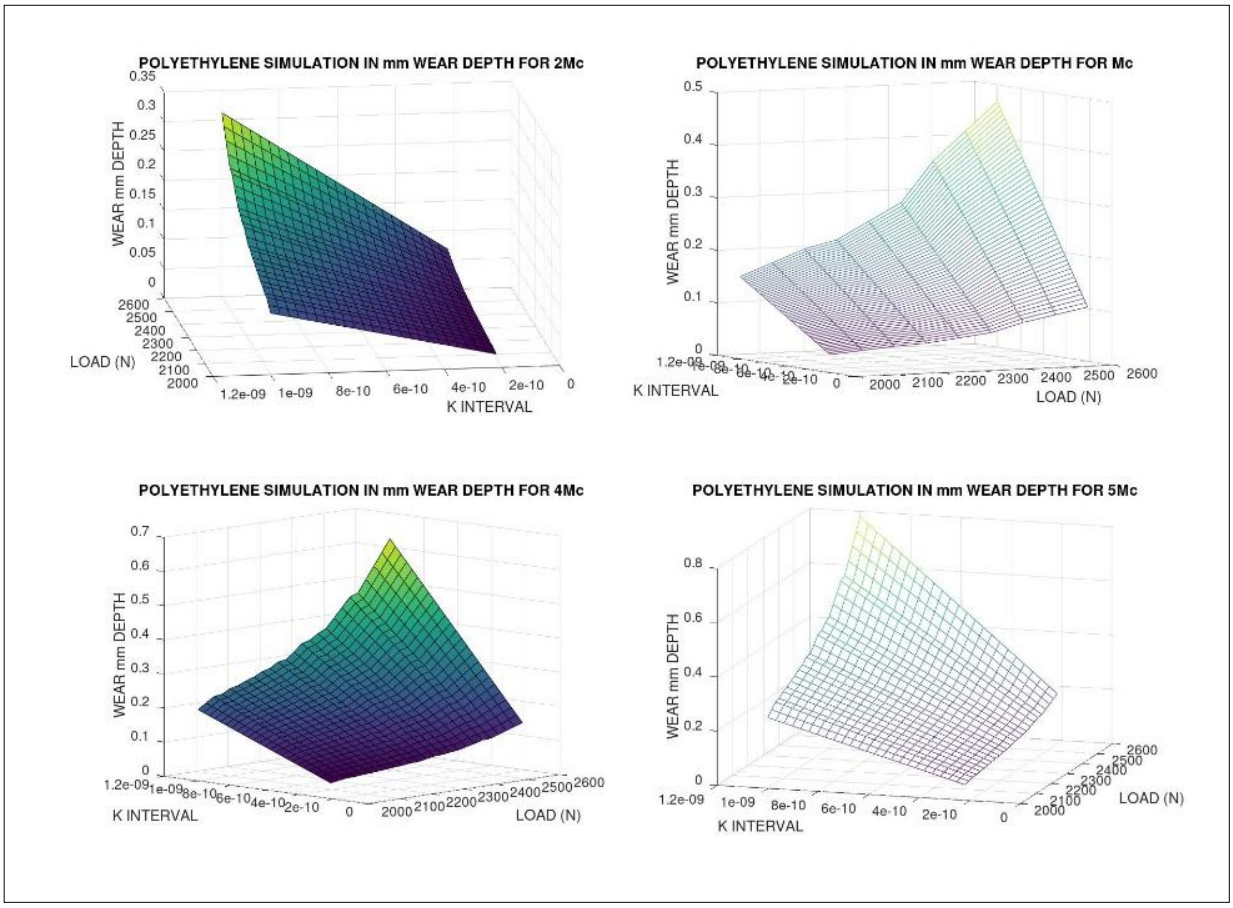

Figure 9.1: Multiple simulation, by using the program of Figure 9, but modified. Two different 3D imaging processing subroutines, with GNU-Octave for (2-5) Mc. It is shown the basic model simulated in mm depth wear (when the surface contact is implemented). It shows the different wear magnitudes when Mc are increasing. The computational method, magnitude-parameters belong to Tables 3-4. GNU-Octave imaging-processing is acceptable. This figure software is also developed in Matlab, Figure 9. [Casesnoves Bioengineering Laboratory Software 2025-k-3]. Note: at figures many times values axe-range of K_w are multiplied by 10^{-3}. This type of software is developed from Author's series of previous publications in hip prostheses wear and other computational contributions [9.33-9.34,9.56].

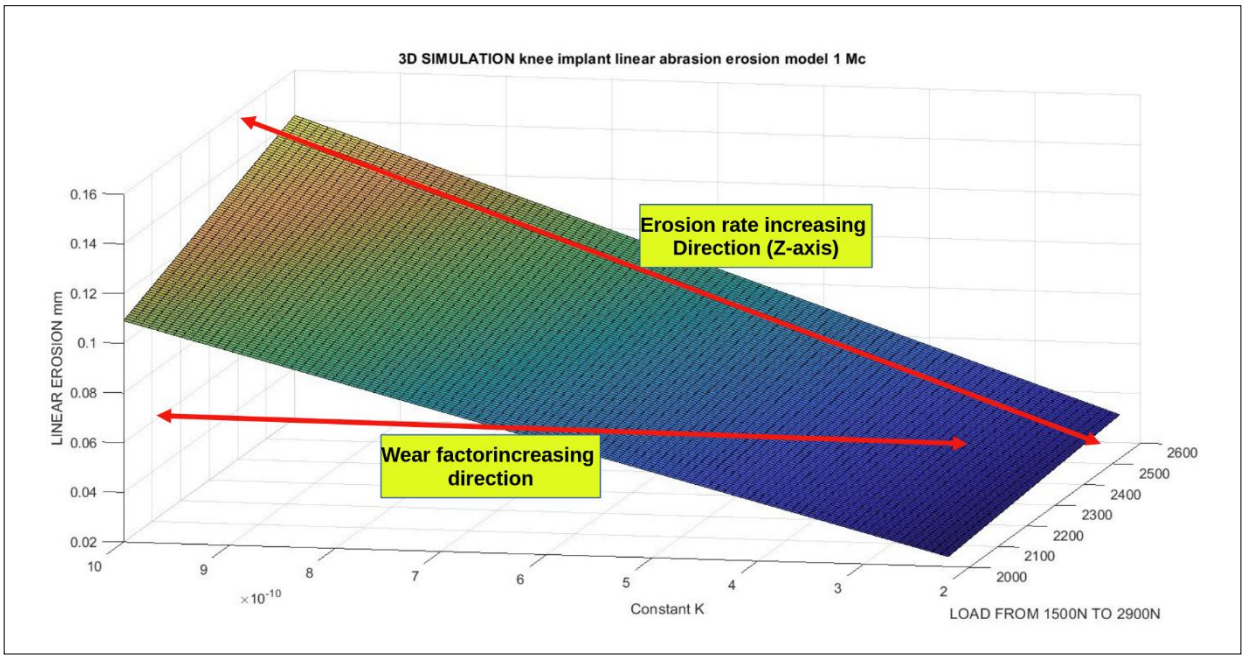

Figure 10: Matlab demonstration with graphical simulation for magnitude changes. It is done with a different/simpler program for 1 Mc. It is shown the basic AM model simulated in wear mm depth. It shows the different wear magnitudes when loads are increasing. [Casesnoves Bioengineering Laboratory Software 2025-k-6].

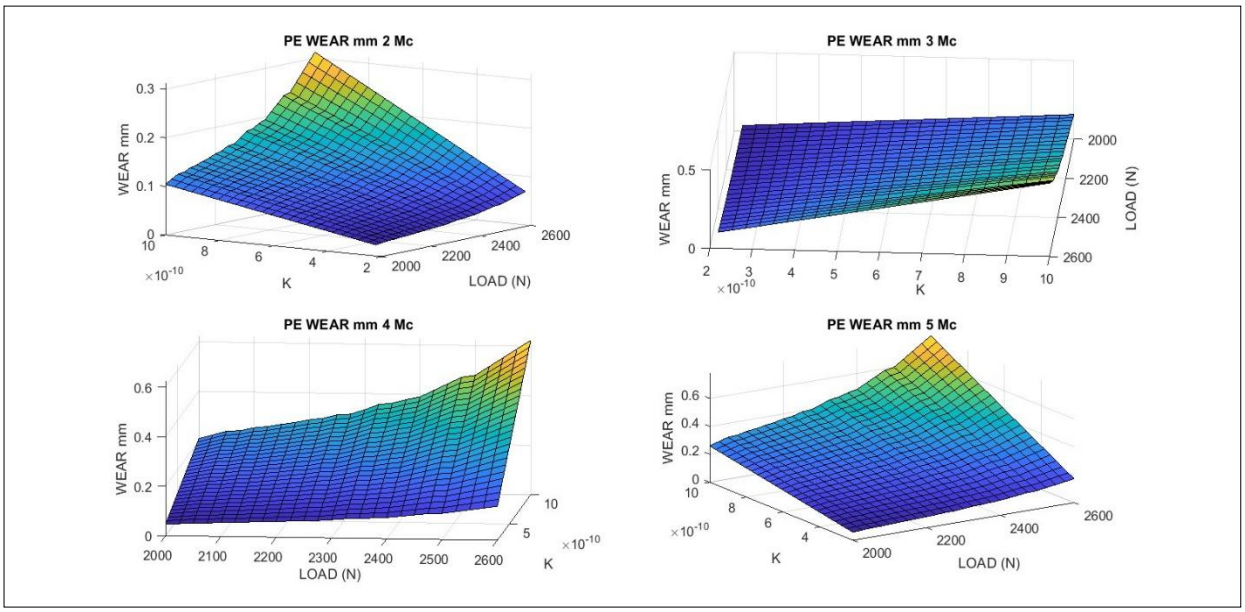

Figure 10.1: Numerical details in multisimulation with Matlab, (2-5 Mc). It is shown the basic model simulated in wear mm depth (when the surface area is implemented). It shows the different wear magnitudes when Mc are increasing. The computational method, magnitude-parameters belong to Tables 3-4, and method to Sketchs 1-2. Note the wear factor K constant magnitude orders. Matlab image-processing is better than GNU-Octave in this case. [Casesnoves Bioengineering Laboratory Software 2025-M-9].

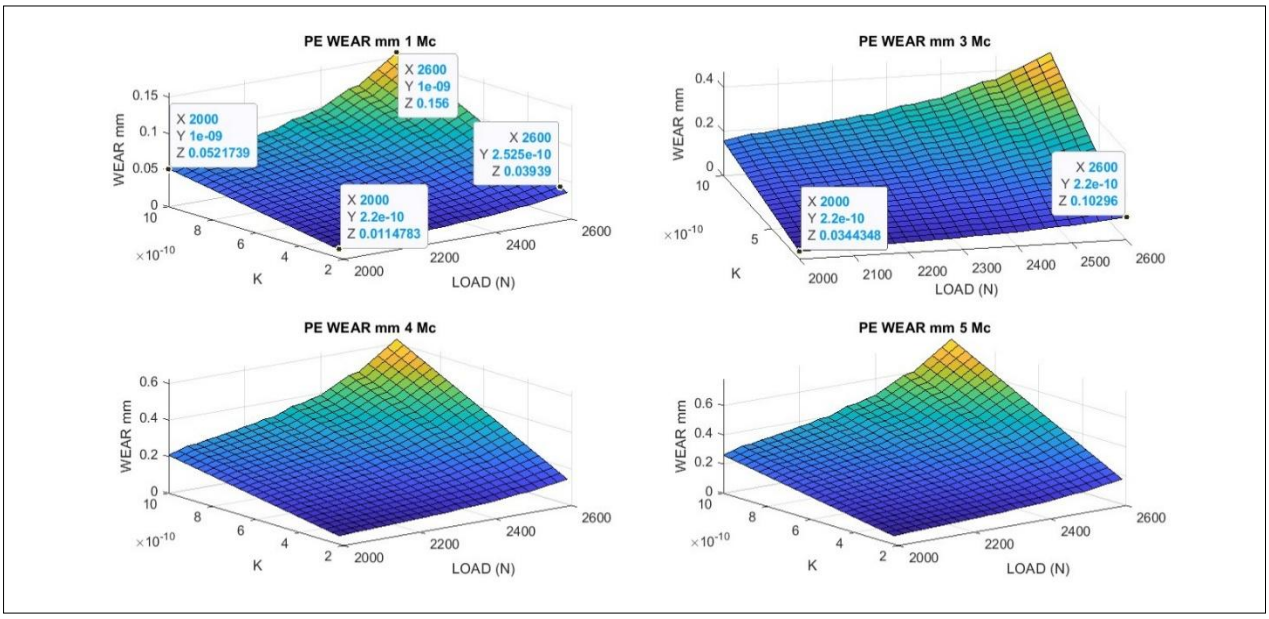

Figure 11: Matlab multisimulation for catching up the differences among 1 Mc and 3,4,5 Mc, it is shown a number of graphical data for multiple simulation with Matlab (dataset of 1,3 Mc included). Image-processing displays the different wear magnitudes when Mc are increasing. Matlab has several 3D imaging processing tools. Matlab image-processing is better than GNU-Octave in this case. [Casesnoves Bioengineering Laboratory Software 2025-k-7]

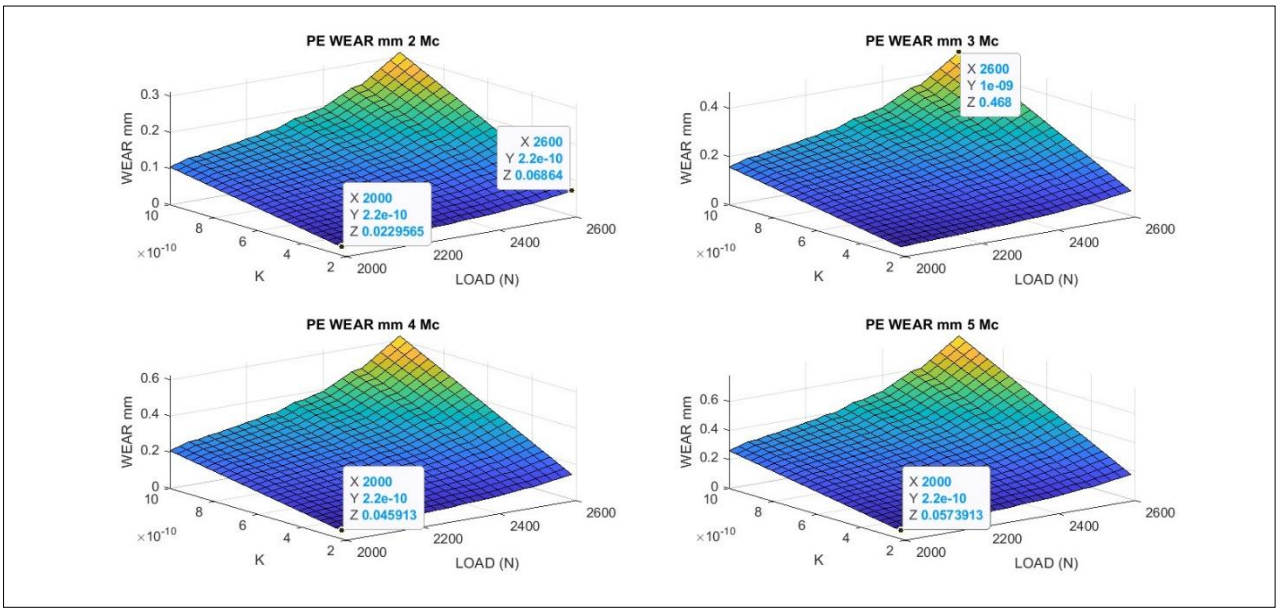

Figure 11.1.- From previous Figures, a number of dataset values implemented at image. That is, a number of graphical data for multiple simulation with Matlab, (2-5 Mc), magnitude values inset. It is shown the basic model simulated in wear mm Depth (When the surface area is implemented). [Casesnoves Bioengineering Laboratory Software 2025-k-5].

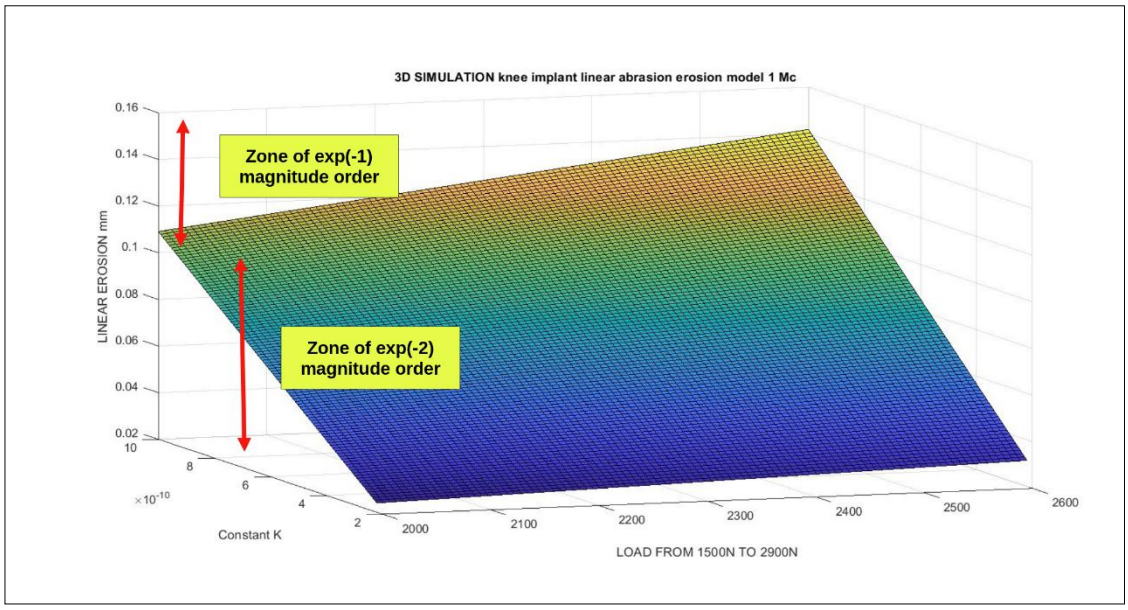

Figure 12: A different perspective for software of Figure 5. Matlab graphical simulation with a simpler program for 1 Mc. It is shown the basic model simulated in wear mm Depth. It is clear the different wear magnitudes when loads are increasing. [Casesnoves Bioengineering Laboratory Software 2025-k-8].

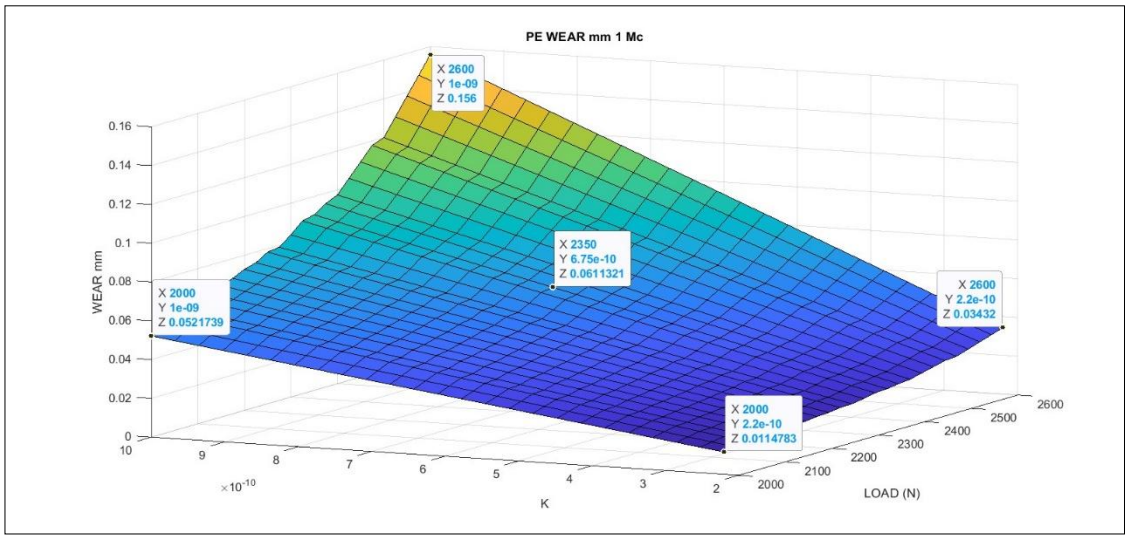

Figure 13: Setting the display of dataset for Figures 12. Matlab program is simple. The dataset inset is used for Tables 5-6 of results. [Casesnoves Bioengineering Laboratory Software 2025-k-9]

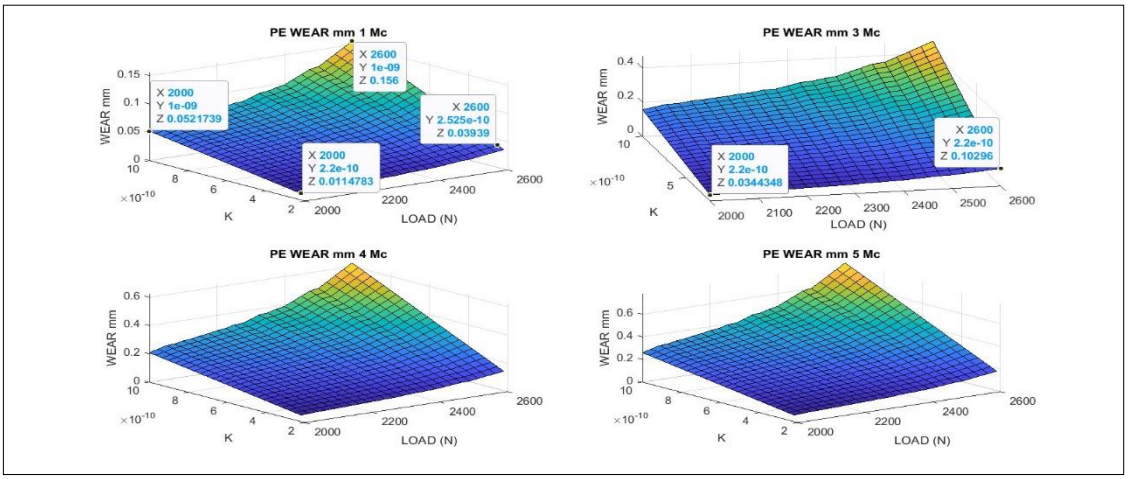

Figure 13.1: For catching up maxima and minima differences among 1 Mc and 3,4,5 Mc, it is shown a number of graphical data for multiple simulation with Matlab (dataset of 1,3 Mc included). Image-processing displays the different wear magnitudes when Mc are increasing. [Casesnoves Bioengineering Laboratory Software 2025-k-7].

7.2 Numerical Results

Graphical Abstract within Table 5 and tabulated magnitudes show extracted from Graphical Optimization the numerical data results for linear wear. Figures and magnitude orders match the standard literature. Those magnitude values can be compared at [8.1-8.32] further references.

ARCHARD MODEL NUMERICAL RESULTS

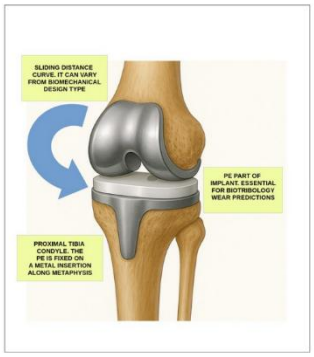

The Archard's Model applied on TKA, integral form proof,

For one cycle,

$$L_{w1} = K_w p S;$$

where S is sliding distance, hence

$$L_{w1} = K_w p v t;$$

therefore, provided $\vec{v}$ constant and taking derivatives for time variable,

$$\frac{dL_{w1}}{dt} = K_w p v; \text{ or,}$$

$$dL_{w1} = K_w p v \, dt, \text{ integrating,}$$

$$\int_0^t dL_{w1} =$$

$$K_w \int_0^t p v \, dt, \text{ supposing instantaneous pressure and sliding velocity during one cycle,}$$

Therefore, taking N cycles, and integrating,

$$L_{wear} = K_{wear} \sum_{j=1}^{N} \sum_{i=1}^{M} \left[\int_0^{t_i} p \, |\vec{v}| \, dt \right]_j ;$$

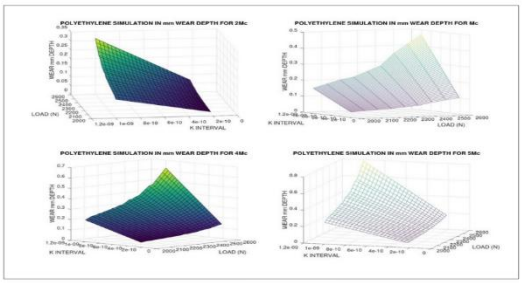

Mc	AM RESULTS MINIMA			AM RESULTS MAXIMA		
	WEAR (mm)	WEAR COEFFICIENT K_w (mm³ / (N x mm)	LOAD (N)	WEAR (mm)	WEAR COEFFICIENT K_w (mm³ / (N x mm)	LOAD (N)
1 Mc	0.01	2.2×10^{-10}	2000	0.16	10^{-9}	2600
2 Mc	0.02	2.2×10^{-10}	2000	0.31	10^{-9}	2600
3 Mc	0.03	2.2×10^{-10}	2000	0.46	10^{-9}	2600
4 Mc	0.05	2.2×10^{-10}	2000	0.62	10^{-9}	2600
5 Mc	0.06	2.2×10^{-10}	2000	0.78	10^{-9}	2600
PRECISION	The mathematical distribution is almost linear for the wear magnitudes.			The mathematical distribution is less linear.		

Table 5: Graphical abstract and main numerical results in the study. Magnitudes match standard literature, [8.1-8.32], Those magnitude values can be compared at [8.1-8.32] further references.

7.3 Comparison of Numerical Results

Graphical abstract within Table 6 presents some numerical comparisons with other literature studies. Some of them are carried out with FE Method, others with FE Method and contrasted with cadaveric data. The most important objective consequence is that from [2,3] Mc on, the Linear Erosion shows a magnitude order jump from 10^{-2} to 10^{-1} mm. The comparisons are shown for database from [8.13-8.17]. However extensive further database can be found at [8.18-8.32].

ARCHARD MODEL COMPARATIVE NUMERICAL RESULTS TO LITERATURE

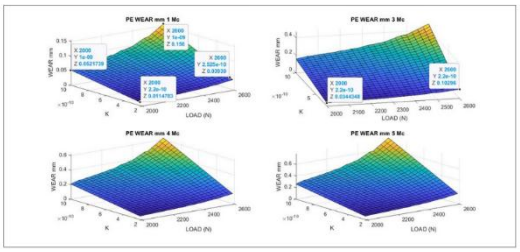

EXTRACT GRAPHICAL DATA → SETTING INTERVALS → COMPARE

Mc [APPROX]	RESULTS APPROXIMATED FOR ALL COMPARISONS CALCULATIONS, WHEN IN VIVO, IT IS TAKEN FROM [8.16], AN AVERAGE OF 2Mc BY YEAR				
	AUTHOR'S STUDY LINEAR WEAR (mm)	1 [8.13,wear+creep,2002] [in vivo, 69 patients, geometrical extrapolation from graphics]	2 [8.14,2019] [in vivo, 49 patients] This author shows dataset for maximum wear, lateral (Lat), and medial (Med). It is shown [ref], Lat=[0.034,0.069]/year, and Med+[0.04,0.069]. All angles. LAT: lateral implant zone MED: medial implant zone	3 [8.15, wear+creep,2019] [in vivo, 106 patients] This Author shows 0.015 mm/year (supine), and 0.220 mm/year (standing). Proportional Average set by this study Author, is calculated here as, (4 x standing+supine) / 5 = 0.1790. Approx=0.18/year.	4 [8.17, 2022] [in vivo-in-vitro, FE compared to 1 cadaveric sample,Flex+AP, geometrical extrapolation from graphics]
1 Mc	[0.01,0.16]	[0.001,0.01]	LAT [0.02, 0.03] MED [0.02,0.03]	[0.09]	[0.03]
2 Mc	[0.02,0.31]	[0.01,0.20]	LAT [0.03,0.07] MED [0.04,0.07]	[0.18]	[0.08]
3 Mc	[0.03,0.46]	[0.50,1.00]	LAT [0.07,0.09] MED [0.06,0.09]	[0.27]	[0.09]
4 Mc	[0.05,0.62]	[1.00,1.10]	LAT [0.08,0.12] MED [0.08,0.12]	[0.36]	[0.10]
5 Mc	[0.06,0.78]	[1.10,1.20]	LAT [0.10,0.15] MED [0.10,0.15]	[0.45]	[0.13]
COMMENTS	Almost linear the wear magnitudes when Mc number is low, proportional to Mc number. Differences tend to get nonlinear in function of Mc, when the Mc magnitude increases.				
IMPORTANT PRECISION	THE WEAR MAGNITUDES AND RATES DIFFER IN LITERATURE AND LABORATORIES FOR TWO MAIN REASONS: (1) THE LARGE VARIETY OF TESTING APPARATUS AND METHODS, (2) THE LARGE VARIETY TO COMMUNICATE/MEASURE RESULTS. NAMELY, WEAR PER Mc (mm), WEAR PER YEAR (mm), WEAR PER Mc (mg), WEAR PER YEAR (mg), AND OTHERS. WHEN THE STUDY IS IN VIVO, WEAR IS USUALLY EXPRESSED IN mm/YEAR. WHAT IS COMMON IS THE POLYETHYLENE DENSITY APPROXIMATELY EQUAL TO WATER [8.13-8.18]. ADDITIONAL COMPLEMENTARY DATASET CAN BE FOUND AT [8.18-8.32].				

Table 6.- Table with Graphical Abstract of AM comparative numerical results. The wear magnitudes and rates differ in literature and laboratories for two main reasons: (1) the large variety of testing apparatus and methods, and the ISO variants also, (2) the large variety to communicate/measure results. Namely, wear per Mc (mm), wear per year (mm),

wear per Mc (mg), wear per year (mg), and others. When the study is in vivo, wear is usually expressed in mm/year, because the in vivo testing takes the sample data usually from patients or recent cadaveric samples whose medical histories show the date when the arthroplasty was done. What is common in all literature, is the polyethylene density approximately equal to water. Magnitude orders match standard literature, [8.3,8.11,8.13-8.18]. Additional complementary dataset can be found at [8.19-8.32]. FE method is used in general for both comparisons/validations with in vivo measurements. Computational Optimization and general Biotribology concepts can be read at [8.33-8.36]. comparisons with other literature studies. Results match in magnitude order these authors dataset.

8. 3D COMPARATIVE-OPTIMIZATION BETWEEN CSM AND AM

Figure 14 shows clearly the linear wear magnitude differences between CSM and AM. However, parameters of second generation models, CSM, have different formulations in the literature. For 1 Mc. There is a maximum difference of 0.15 mm of erosion between AM and CSM. However, these comparative computations will be extended and improved with higher precision in following studies.

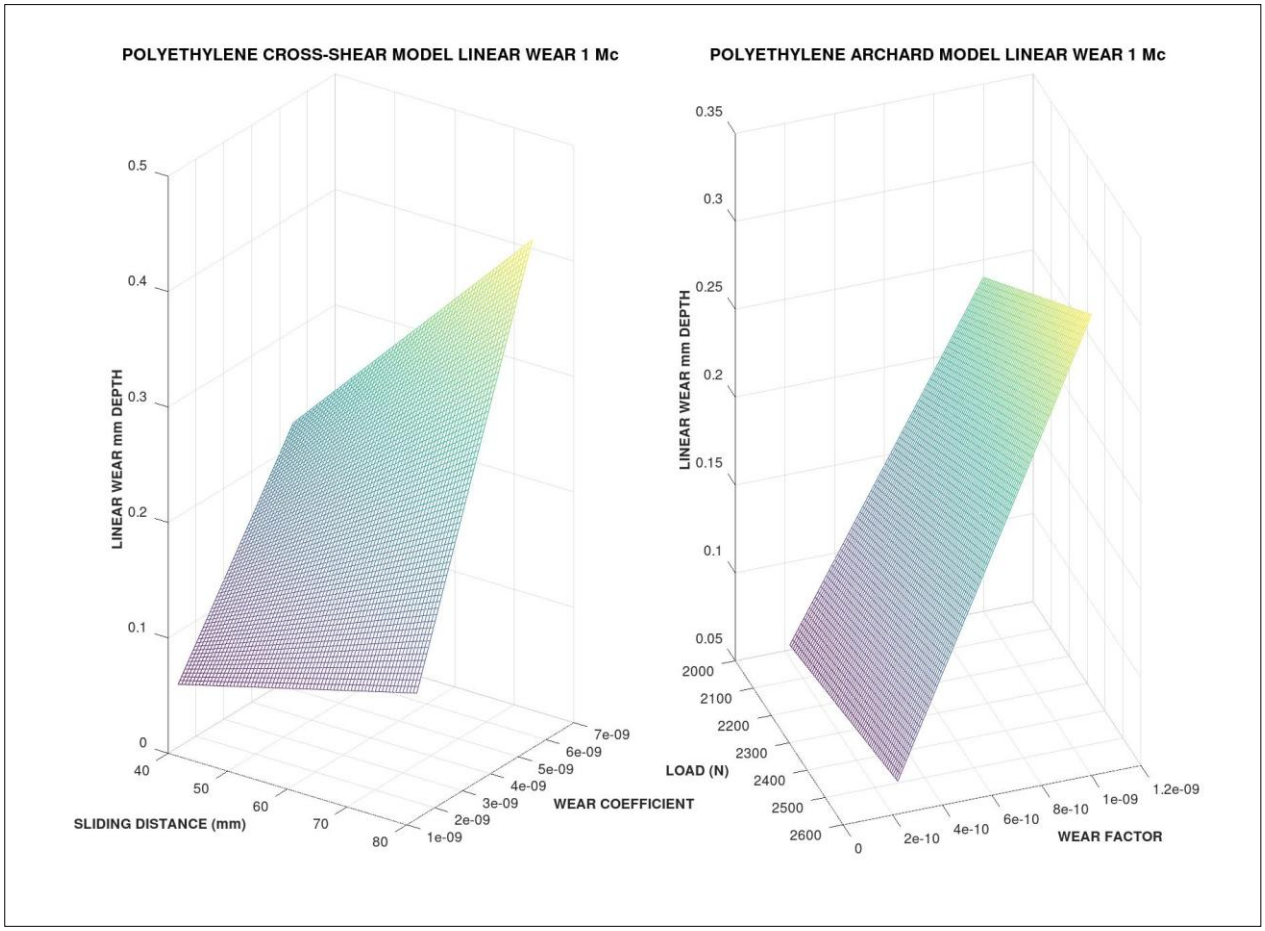

Figure 14: GNU-Octave model system comparative imaging-processing. Note the differences among maxima and minima, for CSM and AM, 1Mc. The computational method, magnitude-parameters belong to Tables 1-3. [Casesnoves Bioengineering Laboratory Software 2025-k-20].

9. BIOMATERIALS AND BIOMECHANICS TKA APPLICATIONS BRIEFING

Table 7 shows a concise concept of study applications. The most important is the erosion rate prediction in order to find approximations for implant durability. Several other applications can be guessed from Table 5.

TKA BIOTRIBOLOGY I+D AND CLINICAL APPLICATIONS	
MANUFACTURING MAIN UTILITY IN COMPUTATIONAL BIOENGINEERING	TKA Wear Predictions and efficacious calculations at 3D image-processing graphs, specially with Matlab, to know the exact magnitude for any selected Wear Coefficient (am), or Wear Factor (CSM model) constants and Load (x, y, coordinates), the approximate predictions of abrasive wear magnitude for 1-5 Mc.
TOTAL WEAR AND BIOTRIBOLOGY BIOMATERIAL PREDICTIONS	For specific UHMWPE material types design/manufacturing of TKA prostheses. TKA erosion prediction, specially for polyethylene materials, is essential, since this polymer is the most widely used in TKA, [8.1-8.32]. Prediction saves manufacturing-research time, repeating laboratory work, and budget.
TKA AVERAGE-DURABILITY PATIENT PREDICTION	Any patient is subject and informed about the lifetime of the TKA implant surgically set. To provide patient with quality of life during implant functional time. What is more, to avoid re-operations and substitution with new prostheses.
BIOMEDICAL INDUSTRIAL MANUFACTURING	The biomedical manufacturing methods are continuously improving. In this line, optimization of manufacturing process and quality improvement is required.
I+D RESEARCH AND CLINICAL RESEARCH	The TKA prostheses are in continuous evolution. For future design of new types. Similar/variants of materials I+D.
PATIENT LIFE QUALITY	Very important for normal movement of patient. Walk and essential movements easy and comfortable for any patient during all duration time.
SPORT MEDICINE ADVANCES	The sport medicine constraint are tougher that common patient conditions. From the average patient knowledge/investigation, progress for sport medicine TKA implants can be got. This is a very important application because sport-medicine requires these prostheses with higher quality than usual patients.

Table 7: Biomechanical and Biotribological applications briefing. Some of them are similar to previous studies in hip joint wear [9.33-9.34]. Further reading and laboratory techniques/applications can be found at [7.1-7.7, 8.1-8.32]

10. DISCUSSION AND CONCLUSIONS

The objectives of the research are to simulate/compare the PE wear without creep models for TKA in a primary approximation. Namely, the Archard's model and the Cross-Shear type. The models applied are initially for linear wear depth. Graphical Optimization for those models, numerical results, and comparison with literature dataset, Tables 1,3,4. Some recipes to develop simulation-software and a briefing applications were included. At this stage, Lubrication Factors for the models were not set.

The graphs obtained are acceptable and abrasive wear numerical results match approximately the standard dataset published, Table 6. For 1 Mc Archard's model abrasive linear wear is of the magnitude order [exp(-2), exp(-1)]. In Cross-Shear type models, the linear wear magnitude is higher, around exp (-1) for 1 Mc, Figures 2-4. For CSM in 1 Mc. There is a maximum difference of 0.15 mm of erosion between AM and CSM. However, these comparative computations will be extended and improved with higher precision in following studies, Figure 14. The proven magnitude jump for AM is presented as much clearly as possible, for example, Illustrative Example 2.

Numerical and graphical optimization results for Archard's model linear wear match the literature ones, Tables 5-6. The cross-shear model results in linear wear are more difficult to compare because at literature, cross-shear models wear magnitudes are shown generally for volumetric wear. Tentative approximations to compare were done dividing the literature volumetric cross-shear magnitudes by an interval of standard contact area, [7.0-7.4]. Just to remark that the cross-shear model investigation line was commenced in this article and will be improved in next contributions.

The image processing quality in GNU-Octave and Matlab is acceptable. It was tried to approach the most common numerical and graphical results published, given the large variety of variants for mathematical models-methods and ISO for abrasive TKA implants predictions.

In brief, a Graphical Simulations-optimizations series for abrasive PE TKA implants with two models were presented. Results for Archard's model linear wear match the literature figures and standards. Applications in Biotribology and Mathematical Optimization-Simulations are presented, Tables 2, 5, 6.

11. SCIENTIFIC ETHICS STANDARDS

All the software was done by Author, based on hip wear previous articles and materials engineering/bioengineering software. The 3D multidigital simulations are original from the Author, software, design, patterns and 3D image processing. The Graphical Optimization software-programs were developed by Author, based on literature, Radiotherapy publications, and previous experience. No artificial intelligence (AI) tools or systems were used for programming anyway. No artificial intelligence (AI) information from browsers was included, and if it would be so, it is always declared. This study was carried out, and their contents are done according to the International Scientific Community and European Union Technology and Science Ethics [9.74-9.76]. References [9.74-9.76]: 'European Textbook on Ethics in Research'. European Commission, Directorate-General for Research. Unit L3. Governance and Ethics. European Research Area. Science and Society. EUR 24452 EN. And based on 'The European Code of Conduct for Research Integrity'. Revised Edition. ALLEA. 2017. When a mathematical statement, algorithm, proposition or theorem is presented, demonstration is always included. When a formula is presented, all parameters are detailed. If any inconsistency is found after publication, it is clarified in subsequent ones. When a citation such as [Casesnoves, 'year'] is set, it is exclusively to clarify intellectual property at current times, without intention to brag. The article is exclusively scientific, without commercial, institutional, academic, religious or religious influences, religious-similar, non-scientific theories, personal opinions, political ideas, or economical influences. When anything is taken from a source, it is adequately recognized.

7. REFERENCES TKA SPECIFIC FOR CROSS-SHEAR MODEL REFERENCES

[7.0] Cho, Y; and Colls; (2025). *Knee Morphology and Proximal Tibial Bone Quality around the Posterior Cruciate Ligament Insertion Site Affect Injury Patterns*. Clinics in Orthopedic Surgery 2025; 17:400-407.

[7.1] Abdelgaied, A; and Colls; (2010). *Computational wear prediction of artificial knee joints based on a new wear law and formulation*. Journal of Biomechanics 44 (2011) 1108–1116. Elsevier.

[7.2] Kang, l: AND Colls; (2008). *Quantification of the effect of cross-shear on the wear of conventional and highly cross-linked UHMWPE*. Journal of Biomechanics 41 (2008) 340–346.

[7.3] Abdelgaied, A; and Colls; (2018). *A comprehensive combined experimental and computational framework for pre-clinical wear simulation of total knee replacements*. Journal of the Mechanical Behavior of Biomedical Materials 78 (2018) 282–291.

[7.4] Shiramizu, K; and Colls; (2009). *Tibiofemoral contact areas and pressures in six high flexion knees*. International Orthopaedics (SICOT) (2009) 33:403–406.

[7.5] Casesnoves, F; (2025). C*omputational simulations-optimization of UHMWPE knee arthroplasty abrasive wear, Second Part*. International Journal of Basic and Applied Medical Sciences ISSN: 2277-2103 Online, International Journal, Available at http://www.cibtech.org/jms.htm 2025 Vol.15, pp. 1-18/ Francisco.

[7.6] Abdelgaied, A; and Colls; (2022). *Understanding the differences in wear testing method standards for total knee replacement*. Journal of the mechanical behavior of biomedical materials 132 (2022) 105258.

[7.7] Haider, H; Garvin K; (2008). *Rotating Platform versus Fixed-bearing Total Knees*. Clin Orthop Relat Res (2008) 466:2677–2685. Springer.

8. REFERENCES TKA GENERAL REFERENCES

[8.1] Dawim, P; (2013). *Biomaterials and medical tribology. Research and development*. Woodhead Publishing. 2013.

[8.2] Schaldach, M; Hohmann, D; (1976). *Advances in artificial hip and knee joint technology*. Springer. 1976.

[8.3] Jin, Z; (2014). *Computational Modelling of Biomechanics and Biotribology in the Musculoskeletal System*. Woodhead Publishing .2014.

[8.4] Munzinger, U; Boldt, J; Keblish, P; (2004). *Primary knee arthroplasty*. Springer 2004.

[8.5] Dawim, P (2010). *Biotribology*. Wiley. 2010.

[8.6] Sculco, T; Martucci, E; (2001). Knee Arthroplasty. Springer. 2001.

[8.7] Emre Tokgoz, E; and Colls; (2023). T*otal Knee Arthroplasty A Review of Medical and Biomedical Engineering and Science Concepts*. Springer. 2023.

[8.8] Kumar, A; and Colls; (2024). *Applications of Biotribology in Biomedical Systems*. Springer. 2024.
[8.9] Kretzer, J; (2014). Wear in total knee arthroplasty—just a question of polyethylene?. International Orthopaedics (SICOT) (2014) 38:335–340. DOI 10.1007/s00264-013-2162-4. 2014.
[8.10] D'Lima, D; (2007). Doctoral Thesis. *In vivo tibial force measurement after total knee arthroplasty*. UC San Diego Electronic Theses and Dissertations. 2007.
[8.11] Affatato, S; (2012). *Wear of orthopaedic implants and artificial joints*. Woodhead Publishing Limited. 2012.
[8.12] Triwardono, J; and Colls; (2021). *Evaluation of the Contact Area in Total Knee Arthroplasty Designed for Deep Knee Flexion*. International Journal of Technology 12(6) 1312-1322 (2021).
DOI: 10.14716/ijtech.v12i6.5193. http://ijtech.eng.ui.ac.id.
[8.13] Hoshino, A; and Colls; (2002). *Accurate in vivo measurement of polyethylene wear in Total Knee Arthroplasty*. The journal of Arthroplasty. Vol 17, No. 4. 2002.
[8.14] Teeter, M; and Colls; (2019). *Radiostereometric analysis permits in vivo measurement of very small levels of wear in TKA*. Clin Orthop Relat Res (2019) 477:80-90. DOI 10.1097/CORR.0000000000000399.
[8.15] Gascoyne, T; and Colls; (2019). *In vivo wear measurement in a modern total knee arthroplasty with model-based radiostereometric analysis*. Bone & Joint Journal 2019;101-B:1348–1355.
[8.16] Silva, M; and Colls; (2002). *Average patient walking activity approaches 2 million cycles per year. pedometers under-record walking activity*. The journal of Arthroplasty. Vol 17, No. 6. 2002.
[8.17] Ozer, A; (2022). *Computational wear of knee implant polyethylene insert surface under continuous dynamic loading and posterior tibial slope variation based on cadaver experiments with comparative verification*. BMC Musculoskeletal Disorders, (2022) 23:871. https://doi.org/10.1186/s12891-022-05828-2 .
[8.18] Heisel, C; and Colls; (2004). *Short-term in vivo wear of cross-linked polyethylene*. The Journal of Bone and Joint Surgery · April 2004. DOI: 10.2106/00004623-200404000-00012. PubMed.
[8.19] Abdelgaied, A; and Colls; (2011). *Computational wear prediction of artificial knee joints based on a new wear law and formulation*. Journal of Biomechanics 44 (2011) 1108–1116. Elsevier. 2011.
[8.20] Pecora, J; Romero, V; (2020). *Evaluation of Polyethylene Wear in a Brazilian Ultracongruent Knee Prosthesis with a Rotating Platform*. Rev Bras Ortop 2021;56(1):42–46. 2021.
[8.21] Soni, A; (2020). *Total Knee Arthroplasty (TKA) Wear Analysis on the Tibial Implant using Finite Element Method Approach*. International Journal of All Research Education and Scientific Methods (IJARESM) ISSN: 2455-6211, Volume 6, Issue 1, January- 2018, Impact Factor: 2.287. 2020.
[8.21.1] Bergmann, G; and Colls (2014). *Standardized Loads Acting in Knee Implants*. PLOS one. January 2014 | Volume 9 | Issue 1 | e86035.
[8.21.2] Dreyer, M; and Colls; (2022). *European Society of Biomechanics S.M. Perren Award 2022: Standardized tibio-femoral implant loads and kinematics*. Journal of Biomechanics 141 (2022) 111171. Elsevier.
[8.22] Innocenti, B; and Colls; (2014). *Development and Validation of a Wear Model to Predict Polyethylene Wear in a Total Knee Arthroplasty: A Finite Element Analysis*. Lubricants 2014, 2, 193-205; doi:10.3390/lubricants2040193. 2014.
[8.23] De Ruiter, L; and Colls; (2020). *The Effects of Cyclic Loading and Motion on the Implant–Cement Interface and Cement Mantle of PEEK and Cobalt–Chromium Femoral Total Knee Arthroplasty Implants: A Preliminary Study*. MDPI. Materials 2020, 13, 3323; doi:10.3390/ma13153323. 2020.
[8.24] Kumar, V; and Colls; (2023). *Triboinformatic Modeling of Wear in Total Knee Replacement Implants Using Machine Learning Algorithms*. Journal of Materials and Engineering Vol. 01, Iss. 3 (2023) 97-105. 2023.
[8.25] Fisher, J; and Colls; (2001). *Wear of polyethylene in artificial knee joints*. Current Orthopaedics (2001) 15, 399d405. Elsevier. 2001.
[8.26] Fuchs, S; and Colls (2000). *Retropatellar contact characteristics in total knee arthroplasty with and without patellar resurfacing*. International Orthopaedics (SICOT) (2000) 24:191–193. Springer.2000.
[8.27] Koh, Y; et al.; (2020). *Prediction of wear performance in femoral and tibial conformity in patient-specific cruciate-retaining total knee arthroplasty*. Journal of Orthopaedic Surgery and Research (2020) 15:24. Journal of Orthopaedic Surgery and Research https://doi.org/10.1186/s13018-020-1548-4 . 2020.
[8.28] Stukenborg-Colsman, C; et al.; (2002). *Tibiofemoral contact stress after total knee arthroplasty*. Acta Orthop Scand 2002; 73 (6):638-646. 2002.
[8.29] Uvehammer, J; (2001). Doctoral Thesis. *Knee joint kinematics, fixation and function related to joint area design in total knee arthroplasty*. Acta Orthopaedica Scandinavica Supplementum no. 299, vol. 72. 2001.

[8.30] A. Abdelgaied, A; Fisher, J; Jennings, L; (2022). *Understanding the differences in wear testing method standards for total knee replacement*. Journal of the Mechanical Behavior of Biomedical Materials 132 (2022) 105258. Elsevier. 2022.
[8.31] Dai, Y; et al.; (2014). *Increased shape and size offerings of femoral components improve fit during total knee arthroplasty*. Knee Surg Sports Traumatol Arthrosc (2014) 22:2931–2940.DOI 10.1007/s00167-014-3163-6. 2014.
[8.32] Fekete, G: et al.; (2017). *Tibiofemoral wear in standard and non-standard squat: implication for total knee arthroplasty*. Muscles, Ligaments and Tendons Journal 2017;7 (4):520-528. 2017.

9. REFERENCES BIOTRIBOLOGY FURTHER READING AND AUTHOR'S HIP ARTHROPLASTY REFERENCES

[9.33] Casesnoves, F; (2021). *Multiobjective Optimization for Ceramic Hip Arthroplasty with Medical Physics Applications*. Int. J. Sci. Res. Comput. Sci. Eng. Inf. Technol. 2021, 7, 582–598. [CrossRef].
[9.33.1] Casesnoves, F; (2021). *Mathematical Multiobjective Optimization for Metal Hip Arthroplasty with Medical Physics Applications*. Journal of Bioscience & Biomedical Engineering. Uniscience Publishers. Wyoming. USA.
[9.33.2] Casesnoves, F; (2021). *Review of Wear Model Optimization for Ceramic and Metal Total Hip Arthroplasty with Medical Physics Applications*. Current Trends Biomedical Eng & Biosci. 2021; 20(2): 556035.
DOI: 10.19080/CTBEB.2021.20.556035. [CrossRef].
[9.33.3] Casesnoves, F; (2022). *Genetic Algorithm to Inverse Least Squares Comparative Dual Optimization for Ceramic Hip Arthroplasty in Medical Physics*. International Journal of Scientific Research in Computer Science, Engineering and Information Technology ISSN: 2456-3307 (www.ijsrcseit.com). DOI: https://doi.org/10.32628/CSEIT2176101 .
[9.33.4] Casesnoves, F; (2021). *Mathematical Standard-Parameters Dual Optimization for Metal Hip Arthroplasty Wear Modelling with Medical Physics Applications*. Standards 2021, 1, 53–66.
https://doi.org/10.3390/standards1010006 . MDPI Institute. [CrossRef].
[9.34] Casesnoves, F; (2018). *Nonlinear comparative optimization for biomaterials wear in artificial implants technology*. In Proceedings of the Applied Chemistry and Materials Science RTU2018 Conference Proceedings, Riga, Latvia, 26 October 2018. [CrossRef].
[9.35] Merola, M.; Affatato, S; (2019). *Materials for Hip Prostheses: A Review of Wear and Loading Considerations*. Materials 2019, 12,495. [CrossRef].
[9.36] Navarro, N; (2008). *Biomaterials in orthopaedics*. J. R. Soc. Interface 2008, 5, 1137–1158. [CrossRef].
[9.37] Kurtz, S; (2014). *Advances in Zirconia Toughened Alumina Biomaterials for Total Joint Replacement*. J. Mech. Behav. Biomed. Mater. 2014, 31, 107–116. [CrossRef].
[9.38] Sachin, G.; Mankar, A.; Bhalerao, Y; (2016). *Biomaterials in Hip Joint Replacement*. Int. J. Mater. Sci. Eng. 2016, 4, 113–125. [CrossRef].
[9.39] Li, Y.; Yang, C.; Zhao, H.; Qu, S.; Li, X.; Li, Y; (2014). *New Developments of Ti-Based Alloys for Biomedical Applications*. Materials 2014, 7, 1709–1800. [CrossRef].
[9.40] Kolli, R.; Devaraj, A; (2018). *A Review of Metastable Beta Titanium Alloys*. Metals 2018, 8, 506. [CrossRef].
[9.41] Holzwarth, U.; Cotogno, G; (2012). *Total Hip Arthroplasty*. JRC Scientific and Policy Reports; European Commission: Brussels, Belgium, 2012.
[9.42] Delimar, D.; (2018). *Femoral head wear and metallosis caused by damaged titanium porous coating after primary metal-on-polyethylene total hip arthroplasty: A case report*. Croat. Med. J. 2018, 59, 253–257. [CrossRef] [PubMed].
[9.43] Zhang, M.; Fan, Y; (2015). *Computational Biomechanics of the Musculoskeletal System.* CRC Press: Boca Raton, FL, USA, 2015.
[9.44] Dreinhöfer, K.; Dieppe, P.; Günther, K.; Puhl, W. Eurohip; (2009). *Health Technology Assessment of Hip Arthroplasty in Europe.* Springer: Berlin/Heidelberg.
[9.45] Casesnoves, F; (2018). *2D computational-numerical hardness comparison between Fe-based hardfaces with WC-Co reinforcements for Integral-Differential modelling*. Trans. Tech. 2018, 762, 330–338. [CrossRef].
[9.46] Hutchings, I.; Shipway, P; (2017). *Tribology Friction and Wear of Engineering Materials, 2nd ed*. Elsevier: Amsterdam, The Netherlands, 2017.
[9.47] Shen, X.; Lei, C.; Li, R; (2010). *Numerical Simulation of Sliding Wear Based on Archard Model*. In Proceedings of the 2010 International Conference on Mechanic Automation and Control Engineering, Wuhan, China, 26–28 June 2010. [CrossRef].
[9.48] Affatato, S.; Brando, D; (2009). *Introduction to Wear Phenomena of Orthopaedic Implants.* Woodhead Publishing: Sawston, UK, 2012.

[9.49] Matsoukas, G.; Kim, Y; (2009). *Design Optimization of a Total Hip Prosthesis for Wear Reduction*. J. Biomech. Eng. 2009, 131, 051003. [CrossRef] [PubMed].
[9.50] Casesnoves, F.; Antonov, M.; Kulo, Pis; (2016). *Mathematical models for erosion and corrosion in power plants. A review of applicable modelling optimization techniques*. In Proceedings of RUTCON2016 Power Engineering Conference, Riga, Latvia, 13 October 2016.
[9.51] Galante, J.; Rostoker, W; (2014). *Wear in Total Hip Prostheses*. Acta Orthop. Scand. 2014, 43, 1–46. [CrossRef] [PubMed].
[9.52] Mattei, L.; DiPuccio, F.; Piccigallo, B.; Ciulli, E; (2011). *Lubrication and wear modelling of artificial hip joints: A review*. Tribol. Int. 2011, 44, 532–549. [CrossRef].
[9.53] Jennings, L; (2012). *Enhancing the safety and reliability of joint replacement implants*. Orthop. Trauma 2012, 26, 246–252. [CrossRef] [PubMed].
[9.54] Casesnoves, F; (2019). *Die Numerische Reuleaux-Methode Rechnerische und Dynamische Grundlagen mit Anwendungen (Erster Teil).* Sciencia Scripts, 2019; ISBN-13 978-620-0-89560-8.
[9.55] Kulu, P.; Casesnoves, F.; Tarbe, R; (2017). *Prediction of abrasive impact wear of composite hardfacings. Solid State Phenomena*. In Proceedings of the 26th International Baltic Conference on Materials Engineering, Vilnius, Lithuania, 26–27 October 2017; Trans Tech Publications: Bäch, Switzerland, 2017; Volume 267, pp. 201–206. [CrossRef].
[9.56] Casesnoves, F; (2018). *Mathematical Models and Optimization of Erosion and Corrosion*. Ph.D. Thesis, Taltech University, Evaluated as excellent, Tallinn, Estonia, 14 December 2018.
[9.57] Saifuddin, A.; Blease, S.; Macsweeney, E; (2003). *Axial loaded MRI of the lumbar spine*. Clin. Radiol. 2003, 58, 661–671. [CrossRef].
[9.58] Damm, P; (2014). *Loading of Total Hip Joint Replacements*. Ph.D. Thesis, Technischen Universität, Berlin.
[9.59] Casesnoves, F; (2019). *The Numerical Reuleaux Method, a Computational and Dynamical Base with Applications. First Part.* Lambert Academic Publishing: Republic of Moldava, 2019; ISBN-10 3659917478.
[9.60] Casesnoves, F; (2007). *Large-Scale Matlab Optimization Toolbox (MOT) Computing Methods in Radiotherapy Inverse Treatment Planning*. High Performance Computing Meeting; Nottingham University: Nottingham, UK, 2007.
[9.61] Casesnoves, F; (2007). *A Monte-Carlo Optimization method for the movement analysis of pseudo-rigid bodies*. In Proceedings of the 10th SIAM Conference in Geometric Design and Computing, San Antonio, TX, USA, 4–8 November 2007. Contributed Talk.
[9.62] Casesnoves, F; (2021). *Theory and Primary Computational Simulations of the Numerical Reuleaux Method (NRM)*. Int. J. Math. Computation 2011, 13, 89–111. Available online: http://www.ceser.in/ceserp/index.php/ijmc/issue/view/119 (accessed on 28 June 2021).
[9.63] Casesnoves, F; (2021). *Applied Inverse Methods for Optimal Geometrical-Mechanical Deformation of Lumbar artificial Disks/Implants with Numerical Reuleaux Method. 2D Comparative Simulations and Formulation*. Comput. Sci. Appl. 2015, 2, 1–10. Available online: www.ethanpublishing.com (accessed on 28 June 2021). Standards 2021, 1.
[9.64] Casesnoves, F; (2018). *Inverse methods and Integral-Differential model demonstration for optimal mechanical operation of power plants–numerical graphical optimization for second generation of tribology models*. Electr. Control Commun. Eng. 2018, 14, 39–50. [CrossRef].
[9.65] Casesnoves, F; Surzhenkov, A; (2017). I*nverse methods for computational simulations and optimization of erosion models in power plants*. In Proceedings of the IEEE Proceedings of RUTCON2017 Power Engineering Conference, Riga, Latvia, 5 December 2017. [CrossRef].
[9.66] Abramobitz, S; (1972). *Handbook of Mathematical Functions*. Appl. Math. Ser. 1972, 55.
[9.67] Luenberger, G; (2005). *Linear and Nonlinear Programming, 4th ed.* Springer: Berlin/Heidelberg.
[9.68] Casesnoves, F; (2016). *Exact Integral Equation Determination with 3D Wedge Filter Convolution Factor Solution in Radiotherapy*. Series of Computational-Programming 2D-3D Dosimetry Simulations. Int. J. Sci. Res. Sci. Eng. Technol. 2016, 2, 699–715.
[9.69] Panjabi, M.; White, A; (1980). *Clinical Biomechanics of the Spine*. Lippincott 1980, 42, S3.
[9.70] Casesnoves, F; (2021). *Software Programming with Lumbar Spine Cadaveric Specimens for Computational Biomedical Applications*. Int. J. Sci. Res. Comput. Sci. Eng. Inf. Technol. 2021, 7, 7–13.
[9.71] Surzhenkov, A.; Viljus, M.; Tarbe, R.; Saarna, M.; Casesnoves, F; (2017). *Wear resistance and mechanisms of composite hardfacings atabrasive impact erosion wear*. J. Phys. 2017, 843, 012060. [CrossRef].

[9.72] Casesnoves, F; (2012). *Computational Simulations of Vertebral Body for Optimal Instrumentation Design. ASME J. Med*. Devices 2012, 6, 021014. [CrossRef].
[9.73] Barker, P; (2014). *The effect of applying tension to the lumbar fasciae on segmental flexion and extension*. In Proceedings of the 5th International Congress of Low Back and Pelvic Pain, Melbourne, Australia, 10–13 November 2014; pp. 50–52.
[9.74] European Textbook on Ethics in Research. European Commission, Directorate-General for Research. Unit L3; (2021). Governance and Ethics. European Research Area. Science and Society. EUR 24452 EN. Available online: https://op.europa.eu/en/publication-detail/-/publication/12567a07-6beb-4998-95cd-8bca103fcf43 (accessed on 28 June 2021).
[9.75] ALLEA; (2017). *The European Code of Conduct for Research Integrity, Revised ed*. ALLEA: Berlin, Germany, 2017.
[9.76] Swedish Research Council. Good Research Practice; (2017). Swedish Research Council: Stockholm, Sweden, 2017. ISBN: 978-91-7307-354-7.

CITATION
Casesnoves, F. (2026). Mathematical-Computational Optimization of UHMWPE Knee Arthroplasty Linear Wear Comparative-Predictions for Archard and Cross-Shear Models. In Global Journal of Research in Engineering & Computer Sciences (Vol. 6, Number 2, pp. 6–39). https://doi.org/10.5281/zenodo.18919268